

From Soft Clustering to Hard Clustering: A Collaborative Annealing Fuzzy c -means Algorithm

Hongzong Li and Jun Wang, *Life Fellow, IEEE*

Abstract—The fuzzy c -means clustering algorithm is the most widely used soft clustering algorithm. In contrast to hard clustering, the cluster membership of data generated using the fuzzy c -means algorithm is ambiguous. Similar to hard clustering algorithms, the clustering results of the fuzzy c -means clustering algorithm are also sub-optimal with varied performance depending on initial solutions. In this paper, a collaborative annealing fuzzy c -means algorithm is presented. To address the issue of ambiguity, the proposed algorithm leverages an annealing procedure to phase out the fuzzy cluster membership degree toward a crispy one by reducing the exponent gradually according to a cooling schedule. To address the issue of sub-optimality, the proposed algorithm employs multiple fuzzy c -means modules to generate alternative clusters based on memberships repeatedly re-initialized using a meta-heuristic rule. Experimental results on eight benchmark datasets are elaborated to demonstrate the superiority of the proposed algorithm to thirteen prevailing hard and soft algorithms in terms of internal and external cluster validity indices.

Index Terms—collaborative clustering; annealing procedure; fuzzy c -means clustering; k -means clustering.

I. INTRODUCTION

CLUSTERING is a popular unsupervised or semi-supervised learning technique to explore the hidden structures of datasets. It is to group unlabeled data into multiple disjoint subsets with high intra-cluster similarity and low inter-cluster similarity. It arises in numerous applications, such as image segmentation [1], information retrieval [1], data mining [1], document clustering [2], video surveillance [2], feature selection [3], and pattern recognition [3].

Over the past decades, numerous clustering algorithms have been proposed, and they are mainly divided into two classes, including hard and soft clustering. Hard clustering is based on the assumption of mutually exclusive clusters, whereas soft clustering relaxes the assumption allowing overlapped clusters. In addition, hard clustering provides a simpler and more straightforward interpretation of the results, whereas soft clustering usually requires further interpretation and analysis to determine appropriate cutoff values for membership assignments.

This work was supported in part by the Research Grants Council of the Hong Kong Special Administrative Region of China under Grants 11202318, 11202019, and 11203721; and in part by the InnoHK initiative, the Government of the Hong Kong Special Administrative Region, and Laboratory for AI-Powered Financial Technologies.

H.-Z. Li and J. Wang are with the Department of Computer Science, City University of Hong Kong, Hong Kong. J. Wang is also with the School of Data Science, City University of Hong Kong, Hong Kong (emails: hongzli2-c@my.cityu.edu.hk, jwang.cs@cityu.edu.hk).

Hard clustering assigns each datum to one and only one cluster. Hard clustering methods may be classified as full-space clustering algorithms, subspace clustering algorithms, feature-weighted clustering algorithms, and multi-view clustering algorithms, depending on the feature spaces of their operations. Subspace clustering methods include the deep subspace clustering algorithm [4] and the robust possibilistic k -subspace clustering algorithm [5]. Feature-weighted clustering methods include the entropy weighting k -means clustering algorithm [6], the entropy-weighted power k -means clustering algorithm [7], and the LASSO-weighted k -means clustering algorithm [8]. Multi-view clustering methods include the weighted multi-view possibilistic c -means clustering algorithm with L2 regularization [9], and the multi-view adjacency-constrained hierarchical clustering algorithm [10]. The hard clustering methods may be classified into hierarchical-based, center-based, distribution-based, and density-based clustering algorithms, according to the structure of the algorithms. Hierarchical-based clustering methods cluster data based on the rule that closer data points exhibit more similarity to each other than the data points lying farther away, including divisive hierarchical algorithms [11] and agglomerative hierarchical algorithms [12]. Center-based clustering methods cluster data based on the rule that similarity is derived by the closeness of data to clusters, including k -means (KM) [13], k -medoids algorithms [14], [15], k -harmonic means [16], and spectral clustering algorithms [17], [18], [19]. Distribution-based clustering methods cluster data based on the probability of data belonging to a specific distribution, including the expectation-maximization for Gaussian mixture model algorithms [20]. Density-based clustering methods cluster data based on the density of data points in the feature space, including the mean-shift algorithm [21], and the temporal streaming fuzzy density-based spatial clustering algorithm [22]. In addition, several collaborative clustering methods are proposed [23], including deep multi-view collaborative clustering [24]. In spite of the progress, the clustering methods cannot guarantee the global optimality of clustering results. To mitigate the difficulty of discontinuity in the underlying objective function of KM, the power k -means (PKM) algorithm clusters data by minimizing the majorization function of an annealed power-mean function [25]. Though the clustering performance using PKM is significantly improved, the clustering result is still sub-optimal and dependent on initialization. To achieve optimal clustering results, the collaborative annealing power k -means++ (CAPKM++) algorithm clusters data by employing multiple PKM modules re-initialized using a particle swarm optimization rule [26]. CAPKM++ is demonstrated to outper-

form PKM and many other baselines [26]. As an upgraded version of CAPKM++, CAPKM++2.0 [27] is shown to be able to improve clustering efficiency via re-initialization during annealing [27].

As a relaxation of hard clustering, soft clustering allows each datum to belong to multiple clusters with membership degrees. Soft clustering methods include possibilistic clustering algorithms [28] and fuzzy clustering algorithms [29]. Possibilistic clustering methods include the robust automatic merging possibilistic clustering algorithm [30], the sparse possibilistic c -means algorithm [31], and the robust possibilistic k -subspace clustering algorithm [5]. Fuzzy clustering methods include the fuzzy c -means algorithm (FCM) [32], the centroid auto-fused hierarchical fuzzy c -means clustering algorithm [33], fuzzy density peaks clustering [34], the robust jointly sparse fuzzy clustering algorithm [35], the fuzzy low-rank structural clustering algorithm [36], and the robust fuzzy c -means algorithm [37]. Soft clustering introduces ambiguity in clustering results due to assigning each data point a membership value to each cluster. In addition, similar to existing hard clustering methods, the results of the soft clustering methods are also sub-optimal.

FCM is one of the popular soft clustering methods due to its efficiency and simplicity [29]. However, it suffers the same drawback as other fuzzy clustering algorithms. To remedy the shortcoming of performance sensitivity to initialization, many alternative methods have been proposed, such as the FCM variants with improved objective function and initialization, and additional constraints. FCM-like algorithms with improved objective function include adaptive fuzzy c -means algorithm [38], generalized fuzzy c -means clustering [39], enhanced FCM [40], fast generalized FCM [41], fuzzy weighted c -means [42], [43], generalized FCM algorithm with improved fuzzy partition [44], fuzzy local information c -means [45], Bayesian fuzzy clustering (BFC) [46], and kernel fuzzy c -means clustering (KFCM) [47]. FCM with improved initialization include multistage random sampling [48], the genetic algorithm [49], the Gustafson-Kessel algorithm [50], initialization schemes by utilizing color space in image segmentation [51], [52], Markov random field [53], and two-phase fuzzy c -means (2PFCM) [54]. Constrained FCM algorithms with additional constraints include the FCM method with spatial constraints [55], [56].

To achieve optimal clustering performance and eliminate the ambiguity in cluster membership and the dependency of performance on initial solutions, we propose the collaborative annealing fuzzy c -means based on FCM (called CAFCM in short). An annealing procedure is used in CAFCM to phase out the fuzziness of cluster membership. In addition, multiple modules are employed to engender alternative clusters and re-initialized repeatedly using a meta-heuristic rule to maximize clustering quality and eliminate the influence of initialization on clustering performance. The innovative contributions of this work are summarized as follows.

- i. We theoretically prove that the underlying objective function of FCM is equivalent to that of PKM without annealing.
- ii. We propose CAFCM with a cooling schedule and experimentally demonstrate that the polynomial cooling

schedule is the most cost-effective one.

- iii. We empirically estimate the computational complexity of CAFCM based on many datasets.
- iv. We experimentally demonstrate that CAFCM outperforms existing hard and soft clustering algorithms in terms of the mean values and standard deviations of many indices.

The remainder of this paper is arranged as follows. The related work on KM, FCM, PKM, CAPKM++, and CAPKM++2.0 is provided in Section II. The details of the CAFCM algorithm are presented in Section III. Experimental results on eight datasets are reported in Section IV. The paper is concluded in Section V.

II. RELATED WORK

A. The KM Algorithm

The KM algorithm is one of the most popular unsupervised learning algorithms. It groups the data into a preset number of clusters by minimizing the following objective function [13]:

$$f(\Theta) = \sum_{i=1}^n \min_{1 \leq j \leq k} \|x_i - \theta_j\|_2^2, \quad (1)$$

where $X = \{x_1, \dots, x_n\} \in \mathbb{R}^{n \times p}$ is an unlabeled dataset, n is the number of data points, k is the number of clusters, p is the number of features, $\Theta = [\theta_1, \dots, \theta_k]$, and $\theta_j \in \mathbb{R}^p$ is the j -th center.

B. The FCM Algorithm

As an extension of KM, FCM was developed by J.C. Dunn [57], and improved by J.C. Bezdek [32]. Differing from KM that assigns each data point to exactly one cluster, FCM allows data points to belong to multiple clusters with different degrees of membership. It is based on the minimization of the following biconvex objective function [32]:

$$f_m(\mu, \Theta) = \sum_{i=1}^n \sum_{j=1}^k \mu_{ij}^m \|x_i - \theta_j\|^2, \quad (2)$$

where $\mu_{ij} \in [0, 1]$ is the degree of membership of the i -th datum in the j -th cluster, $m > 1$ is an exponent for controlling the degree of fuzzy overlap, and θ_j is the center of the j -th cluster. The fuzzy objective function is subject to a constraint $\sum_{j=1}^k \mu_{ij} = 1$ ($i = 1, \dots, n$); i.e., for each datum, the sum of the membership degrees over all clusters is one.

The centers are updated as follows [32]: for $j = 1, \dots, k$,

$$\theta_j = \frac{\sum_{i=1}^n \mu_{ij}^m x_i}{\sum_{i=1}^n \mu_{ij}^m}. \quad (3)$$

The degrees are updated alternately as follows [32]: for $i = 1, \dots, n$ and $j = 1, \dots, k$,

$$\mu_{ij} = \frac{1}{\sum_{l=1}^k \left(\frac{\|x_i - \theta_j\|}{\|x_i - \theta_l\|} \right)^{\frac{2}{m-1}}}. \quad (4)$$

Similar to KM, FCM iterates over (3) and (4) until no degree changes. Due to the biconvexity of the fuzzy objective function

in (2), the alternating method cannot guarantee to converge to the global optimal cluster.

Note that $\lim_{m \rightarrow 1} \mu_{ij} \in \{0, 1\}$; i.e., FCM degenerates to KM [29].

C. The PKM Algorithm

PKM [25] is proposed to improve k -means algorithms by minimizing the following annealed power function:

$$f_s(\Theta) := \sum_{i=1}^n \left(\frac{1}{k} \sum_{j=1}^k \|x_i - \theta_j\|_2^{2s} \right)^{\frac{1}{s}}, \quad (5)$$

where $s < 0$ denotes a power parameter.

Rather than minimizing the concave power-mean functions in (5), PKM minimizes the convex majorization function [25]:

$$\hat{f}_s(\Theta) = \sum_{i=1}^n \sum_{j=1}^k w_{ij}(t) \|x_i - \theta_j(t+1)\|_2^2. \quad (6)$$

The weights are updated as follows [25]:

$$w_{ij}(t) = \frac{\|x_i - \theta_j(t)\|_2^{2(s-1)}}{(\sum_{l=1}^k \|x_i - \theta_l(t)\|_2^{2s})^{1-\frac{1}{s}}}. \quad (7)$$

The clusters are updated as follows [25]:

$$\theta_j(t+1) = \frac{1}{\sum_{i=1}^n w_{ij}(t)} \sum_{i=1}^n w_{ij}(t) x_i.$$

The power parameter s is decreased at each step according to the following cooling schedule [25]:

$$s(t+1) = \eta s(t),$$

where $s(0) < 0$ and $\eta > 1$.

Let $s = -\frac{1}{m-1}$. The weight updating rule in (7) is rewritten as follows:

$$\begin{aligned} w_{ij} &= \frac{\|x_i - \theta_j\|_2^{2(s-1)}}{(\sum_{l=1}^k \|x_i - \theta_l\|_2^{2s})^{1-\frac{1}{s}}}, \\ &= \frac{\|x_i - \theta_j\|_2^{-2m/(m-1)}}{(\sum_{l=1}^k \|x_i - \theta_l\|_2^{-2/(m-1)})^m}. \end{aligned} \quad (8)$$

Via substituting the weight updating rule in (8), the objective function in (5) is rewritten as follows:

$$\begin{aligned} \hat{f}_s(\Theta) &= \sum_{i=1}^n \sum_{j=1}^k w_{ij} \|x_i - \theta_j\|_2^2, \\ &= \sum_{i=1}^n \sum_{j=1}^k \frac{\|x_i - \theta_j\|_2^{-2m/(m-1)}}{(\sum_{l=1}^k \|x_i - \theta_l\|_2^{-2/(m-1)})^m} \|x_i - \theta_j\|_2^2, \end{aligned} \quad (9)$$

The degree updating rule of FCM in (4) is rewritten as follows:

$$\begin{aligned} \mu_{ij} &= \frac{1}{(\sum_{l=1}^k (\frac{\|x_i - \theta_j\|_2}{\|x_i - \theta_l\|_2})^{\frac{2}{m-1}})}, \\ &= \frac{\|x_i - \theta_j\|_2^{-2/(m-1)}}{\sum_{l=1}^k (\|x_i - \theta_l\|_2)^{2/(m-1)}}, \end{aligned} \quad (10)$$

Via substituting the degree updating rule in (10), the objective function of FCM in (2) is further rewritten as follows:

$$\begin{aligned} f_m(\mu, \Theta) &= \sum_{i=1}^n \sum_{j=1}^k \mu_{ij}^m \|x_i - \theta_j\|_2^2, \\ &= \sum_{i=1}^n \sum_{j=1}^k \frac{\|x_i - \theta_j\|_2^{-2m/(m-1)}}{(\sum_{l=1}^k \|x_i - \theta_l\|_2^{-2/(m-1)})^m} \|x_i - \theta_j\|_2^2, \end{aligned} \quad (11)$$

It indicates that the objective functions of FCM in (9) and PKM in (11) are equivalent.

D. The CAPKM++ and CAPKM++2.0 Algorithms

PKM is demonstrated in [25] to perform better than Lloyd's algorithm [13] and k -harmonic means [16]. Nevertheless, its clustering results are not globally optimal since its performance heavily depends on the anchor points where its majorization functions are located. To address the aforementioned issue, CAPKM++ [26] employs multiple PKM modules to generate centers for alternative clusters, and use a particle swarm optimization rule for repositioning the initial centers.

CAPKM++2.0 [27] is an upgraded version of CAPKM++. CAPKM++2.0 re-initializes the weights in the majorization function during annealing rather than re-initializing cluster centers after annealing. Additionally, CAPKM++2.0 minimizes the power-mean functions directly instead of their majorization function as in PKM and CAPKM++. It is demonstrated in [27] that CAPKM++2.0 is more efficient than CAPKM++ in terms of algorithmic complexities.

III. ALGORITHM DESCRIPTION

The proposed CAFCM algorithm consists of triple loops: an FCM clustering loop, a reinitialization loop, and an annealing loop. In the FCM clustering loop, multiple FCM modules iterate until convergence. In the reinitialization loop, the FCM modules are reinitialized. In the annealing loop, an exponent $m(t)$ decreases iteratively. The fuzzy objective function in (2) is minimized during such an annealing process, similar to PKM [25], CAPKM++ [26], and CAPKM++2.0 [27]. As shown in Fig. 1, the following three types of cooling schedules may be used for the annealing of exponent $m(t)$. An exponential cooling schedule:

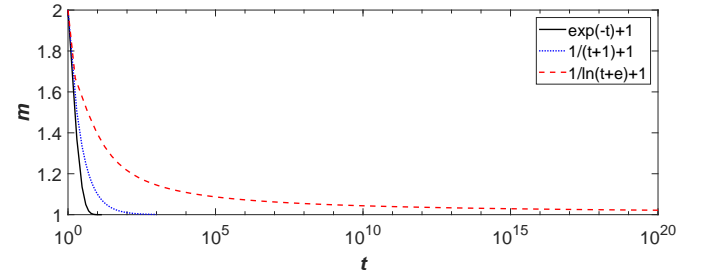


Fig. 1. The annealing curves of the three cooling schedules.

$$m_e(t) = (m_e(0) - 1) \exp(-t) + 1. \quad (12)$$

A polynomial cooling schedule:

$$m_p(t) = \frac{m_p(0) - 1}{t + 1} + 1. \quad (13)$$

A logarithmic cooling schedule:

$$m_l(t) = \frac{m_l(0) - 1}{\ln(t + e)} + 1. \quad (14)$$

Note that $\lim_{t \rightarrow \infty} m_e(t) = \lim_{t \rightarrow \infty} m_p(t) = \lim_{t \rightarrow \infty} m_l(t) = 1$. Each of the three cooling schedules has its pros and cons. As shown in Fig. 1, the exponential cooling schedule is the fastest, and it may cause prematurity in analogy to simulated annealing. The logarithmic cooling schedule is the slowest, and it takes a very long time to reduce to 1. The polynomial schedule is in-between.

In analogy to CAPKM++ [26] and CAPKM++2.0 [27], to overcome the biconvexity, $\mu(0)$ is repeatedly re-initialized according to the following particle swarm optimization rule in [58]:

$$v^{(i)}(t+1) = c_0 v^{(i)}(t) + c_1 r_1 (\mu^{(i)*} - \mu^{(i)}(t)) \quad (15a)$$

$$+ c_2 r_2 (\mu^* - \mu^{(i)}(t)), \quad (15b)$$

$$\mu^{(i)}(t+1) = \mu^{(i)}(t) + v^{(i)}(t+1), \quad (15c)$$

where $v^{(i)}(t)$ is an incremental vector of the i -th module, $\mu^{(i)*}$ is the current best degree vector of the i -th module, $\mu^{(i)}(t)$ is the current degree vector of the i -th module, μ^* is the current best degree vector of the multiple modules, $c_0 \in [0, 1]$ is a constant, c_1, c_2 are two positive constants, and r_1, r_2 are two random numbers in $[0, 1]$.

The high diversity of solutions is essential for improving clustering performance. A diversity measure of solutions is defined as follows:

$$\delta(\mu) = \frac{1}{Nnk} \sum_{j=1}^N \|\mu^{(j)} - \mu^*\|_2, \quad (16)$$

where N is the population size (i.e., the number of alternative cluster sets).

Mutation operation is a commonly used method to maintain a certain level of diversity and prevent premature convergence. If the diversity measure is below a threshold (i.e., $\delta(\mu) < \delta_{\min}$), then a wavelet mutation operator is used to assure the diversity [59]:

$$\mu^{(i)}(t+1) = \begin{cases} \mu^{(i)}(t) + \zeta(\bar{\mu}^{(i)} - \mu^{(i)}(t)) & \zeta > 0, \\ \mu^{(i)}(t) + \zeta(\underline{\mu}^{(i)} - \mu^{(i)}(t)) & \zeta < 0, \end{cases} \quad (17)$$

where $\bar{\mu}^{(i)} = 1$ and $\underline{\mu}^{(i)} = 0$ are the upper bound and lower bound of the membership degree of the i -th module, and ζ is defined by a wavelet function:

$$\zeta = \frac{1}{\sqrt{a}} \exp - \frac{1}{2} \left(\frac{\psi}{a} \right)^2 \cos \left(\frac{5\psi}{a} \right),$$

where $a = \exp(10(\ell/\ell_{\max}))$ is the amplitude of the wavelet function, ℓ_{\max} is the maximum iterative number, and ψ is the frequency of the wavelet function to be randomly generated from the interval $[-2.5a, 2.5a]$.

Figure 2 portrays a flowchart of the CAFCM algorithm, and Algorithm 1 details its procedure. In Steps 6-10, centers Θ and

Algorithm 1: CAFCM

Input: $M, N, m(0), c_0, c_1$ and $c_2, X \in \mathbb{R}^{n \times p}$.
particle/group best degrees $\tilde{\mu}^{(p)}/\mu^*$,
 $f(\tilde{\mu}^{(p)}) = f(\mu^*) = \infty$, initial degrees
 $[\mu^{(1)}(0), \dots, \mu^{(N)}(0)]$, initial incremental vector
 $[v^{(1)}(0), \dots, v^{(N)}(0)]$,
Output: μ^* .

```

1  $t \leftarrow 0$ ;
2 repeat
3   while  $l \leq M$  do
4     for  $i = 1$  to  $N$  do
5        $\hat{t} \leftarrow 1$ ;
6       repeat
7         Update  $\Theta^{(i)}(\hat{t})$  according to Eqn. (3);
8         Update  $\mu^{(i)}(\hat{t})$  according to Eqn. (4);
9          $\hat{t} \leftarrow \hat{t} + 1$ ;
10      until  $|f_m(\mu^{(i)}(\hat{t}), \Theta^{(i)}(\hat{t})) - f_m(\mu^{(i)}(\hat{t} - 1), \Theta^{(i)}(\hat{t} - 1))| < \epsilon$ ;
11      if  $f(\mu^{(i)}) < f(\tilde{\mu}^{(i)})$  then
12         $\tilde{\mu}^{(i)} \leftarrow \mu^{(i)}$ ;
13      end
14    end
15     $i^* = \arg \min_i \{f(\mu^{(1)}), \dots, f(\mu^{(i)}), \dots, f(\mu^{(N)})\}$ ;
16    if  $f(\mu^{(i^*)}) < f(\mu^*)$  then
17       $\mu^* \leftarrow \mu^{(i^*)}$ ;
18       $l \leftarrow 0$ ;
19    else
20       $l \leftarrow l + 1$ ;
21    end
22    for  $i = 1$  to  $N$  do
23      Update  $v^{(i)}$  according to Eqn. (15a);
24      Update  $\mu^{(i)}$  according to Eqn. (15c);
25    end
26    Compute  $\delta(\mu)$  according to Eqn. (16);
27    if  $\delta(\mu) < \delta_{\min}$  then
28      Perform mutation according to Eqn. (17);
29    end
30  end
31   $t \leftarrow t + 1$ ;
32  Reduce  $m(t)$  according to Eqn. (12), Eqn. (13), or Eqn. (14);
33 until  $m(t) - 1 < \epsilon$ ;
34 return  $\mu^*$ .

```

degrees μ are updated alternately until convergence, where ϵ in Step 10 is to determine whether $f_m(\mu^{(i)}(\hat{t}), \Theta^{(i)}(\hat{t}))$ and $f_m(\mu^{(i)}(\hat{t} - 1), \Theta^{(i)}(\hat{t} - 1))$ are close enough. In Steps 11-13, the individual best degrees $\tilde{\mu}^{(i)}$ are determined. In Steps 15-21, the group best degrees μ^* are determined and the termination counter is updated. In Steps 22-25, the degrees are re-initialized according to (15). In Step 26, the diversity of the N sets of degrees is measured according to (16). In Steps 27-29, the wavelet mutation operator in (17) is performed if the diversity measure is below the preset threshold δ_{\min} . In Step 32, the exponent m is reduced according to one of the

three cooling schedules. In Step 10, the termination condition whether m is close to 1 is determined. The code of CAFCM is available in Github¹.

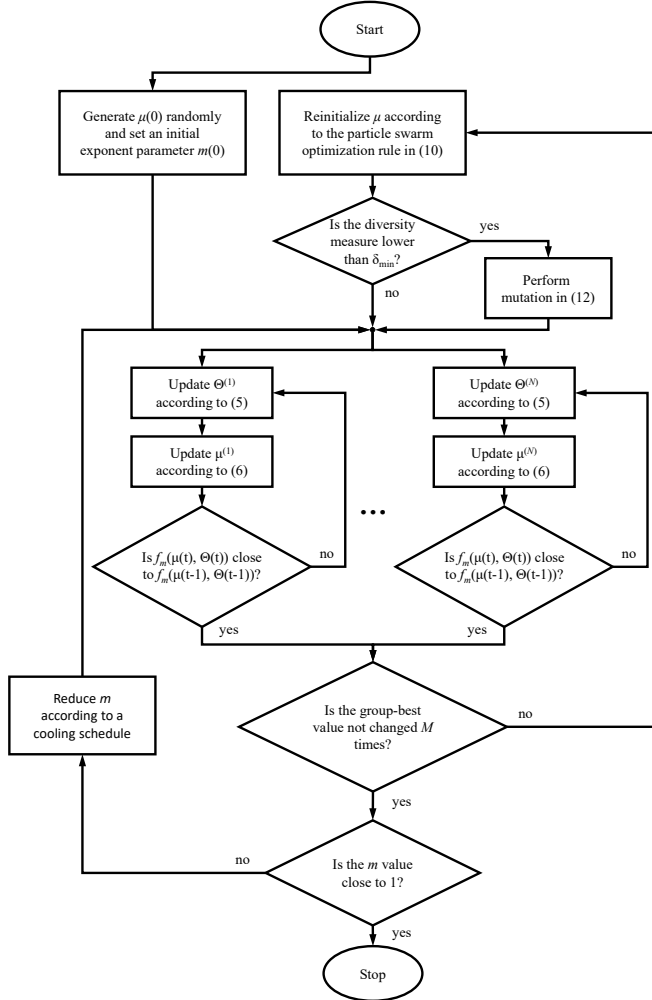


Fig. 2. A flowchart of CAFCM.

IV. EXPERIMENTAL RESULTS

In the experiments, the CAFCM parameters are set as follows. The value of the initial exponent $m(0)$ is set to 2, as in most of the existing references. The diversity threshold δ_{\min} is set to a sufficiently small value (i.e., 10^{-3}). In the FCM clustering loop of CAFCM, the parameter ϵ is also set to a sufficiently small value (i.e., 10^{-3}) as a stopping criterion of cluster membership updating. In the particle swarm optimization rule in (15), c_0 , c_1 , and c_2 are set to 1, as typically in many references; e.g., [26], [27].

A. Cooling Schedules

In this subsection, we compare the performances of CAFCM with the three cooling schedules. To make a fair comparison, the three cooling schedules are set to the same number of iterations. Since the logarithmic cooling schedule takes a long

time for $m(t)$ to reduce to 1, instead of iterating over every t , sampling time $\tau(t)$ is used under the condition that the value of $m_l(\tau)$ is larger than that of the polynomial cooling schedule at every sampling time (i.e., $m_l(\tau(t)) > m_p(t)$) to keep its annealing process slower than the polynomial one. Since $\frac{m_p(0)}{t+2} > \frac{m_p(0)-1}{t+1}$ for $t > m_p(0) - 1$, letting $\frac{m_l(0)-1}{\ln(\tau(t)+e)} + 1 = \frac{m_p(0)}{t+2} + 1$ enables $m_l(\tau(t)) > m_p(t)$. The solution to the equation is $\tau(t) = \exp(\frac{(m_l(0)-1)(t+2)}{m_l(0)}) - e$, assuming that $m_l(0) = m_p(0)$.

The experimental results are based on eight commonly used datasets summarized in Table I. In addition, to show the superiority of CAFCM with the logarithmic cooling schedule on the dataset that is difficult to cluster, a dataset under uniform distribution (called UDD) is generated, where $n = 5000$ and $p = 2$.

TABLE I
INFORMATION ABOUT THE EIGHT BENCHMARK DATASETS AND THE CORRESPONDING HYPER-PARAMETER VALUES USED IN CAFCM.

Datasets	n	p	k	N	M
NCI9 ¹ [60]	60	9712	9	2	10
WarpPIE10P ² [60]	210	2420	10	2	5
WQ-White ³ [61]	4898	11	11	2	15
PageBlocks ⁴ [61]	5472	10	5	2	5
Texture ⁵ [61]	5500	40	11	3	15
Optdigits ⁶ [61]	5620	65	10	2	5
EGS ⁷ [62]	10000	13	2	2	5
LR ⁸ [63]	20000	16	26	3	15

¹ <https://jundongli.github.io/scikit-feature/files/datasets/nci9.mat>

² <https://jundongli.github.io/scikit-feature/files/datasets/warpPIE10P.mat>

³ <https://sci2s.ugr.es/keel/dataset.php?cod=209>

⁴ <https://sci2s.ugr.es/keel/dataset.php?cod=104>

⁵ <https://sci2s.ugr.es/keel/dataset.php?cod=72>

⁶ <https://sci2s.ugr.es/keel/dataset.php?cod=199>

⁷ <https://archive.ics.uci.edu/ml/datasets/Electrical+Grid+Stability+Simulated+Data+>

⁸ <https://archive.ics.uci.edu/ml/datasets/Letter+Recognition>

Fig. 3 shows 20-run Monte Carlo test results of CAFCM ($N = 2$ and $M = 5$) with the three cooling schedules on the six datasets in Table I and the uniformly distributed dataset. As shown in Fig. 3, CAFCM with the polynomial cooling schedule or the logarithmic cooling schedule outperforms that with the exponential cooling schedule. It is also shown in Fig. 3 that CAFCM with the logarithmic cooling schedule outperforms that with the polynomial cooling schedule on NCI9, Texture, and UDD, especially on the uniformly distributed dataset, and the superiority is more evident for a larger k value on the uniformly distributed dataset.

Although the performance of CAFCM with the logarithmic cooling schedule is better than that with the polynomial cooling schedule, it takes too long time to reach 1, or it is difficult to set a reasonable sampling time to achieve high performance. In the view that CAFCM with the polynomial cooling schedule performs well on the six datasets in Table I, the polynomial cooling schedule $m_p(t)$ is used in all the other experiments.

¹ <https://github.com/HongzongLI-CS/CAFCM-Github>

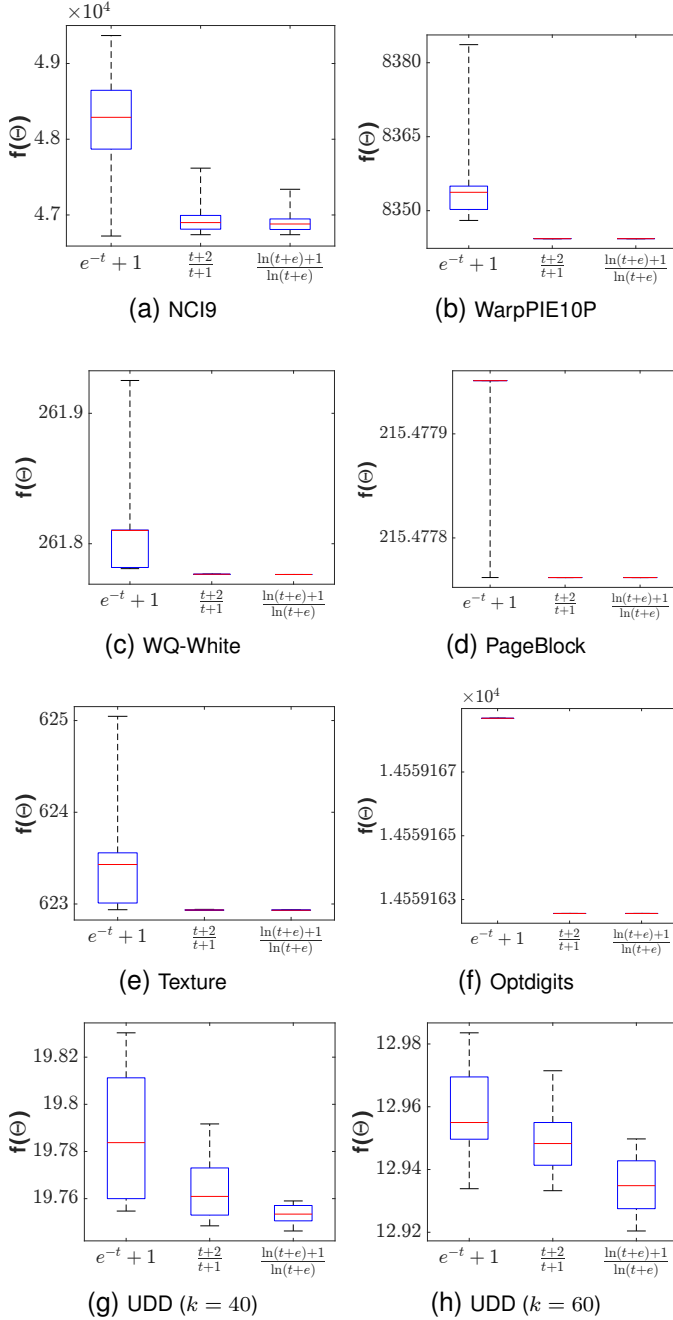


Fig. 3. Monte Carlo test results of CAFCM ($N = 2$ and $M = 5$) with the three cooling schedules on the six datasets and the uniformly distributed dataset with two different k values.

B. Hyper-parameters Selection

Similar to CAPKM++ [26] and CAPKM++2.0 [27], the values of two hyper-parameters N and M in Algorithm 1 are selected based on 50-run Monte Carlo tests on the six datasets. Fig. 4 depicts the boxplots of the Monte Carlo test results obtained using the CAFCM algorithm over 20 runs on the six datasets. As shown in Fig. 4, the results of the objective function values reaching zero standard deviation with $N = 2$ and $M = 10$ on NCI9, $N = 2$ and $M = 5$ on WQ-White, $N = 2$ and $M = 15$ on WarpPIE10P, $N = 2$ and $M = 5$ on PageBlocks, $N = 3$ and $M = 15$ on Texture, and $N = 2$

and $M = 5$ on Optdigits. Table I tabulates the values of the two hyper-parameters (i.e., N and M) used in CAFCM on the eight datasets.

C. Convergent Behaviors

Fig. 5 depicts twelve snapshots of the convergent centers Θ and the convergent degrees μ values in the FCM clustering loop (Steps 6-10) of CAFCM on the six datasets. Fig. 6 depicts the monotonically decreasing values of $f_m(\mu, \Theta)$ in Eqn. (2) corresponding to Θ and μ in Fig. 5. They show that the centers and the degrees reach their equilibria and the fuzzy objective function values reach their minima with a range of 40-400 iterations in the FCM clustering loop of CAFCM.

Fig. 7 depicts the monotonically decreasing values of $f(\Theta)$ in the annealing loop (Steps 2-33) of CAFCM on the six datasets. It shows that CAFCM converges within 120 iterations on NCI9, 80 iterations on WarpPIE10P, 1000 iterations on WineQuality-White, 30 iterations on PageBlocks, 160 iterations on Texture, and 1500 iterations on Optdigits.

D. Performance Comparison

The clustering performance of CAFCM is compared with the following six fuzzy clustering algorithms and seven crisp clustering algorithm: KM^2 , k -mean++ ($KM++$)³, PKM [25], entropy weighted power k -means (EWPKM)⁴, spectral clustering (SC)⁵, hierarchical clustering (HC)⁶, CAPKM++2.0 [27], BFC [46], fuzzy subspace clustering (FSC) [64], maximum entropy clustering (MEC) [65], FCM⁷, KFCM [47], and 2PFCM [54]. The clustering results of the fuzzy clustering algorithms (i.e., BFC, FSC, MEC, FCM, KFCM, and 2PFCM) are determined by the maximum fuzzy membership degrees. The code of PKM is provided by the authors of [25]. The agglomerative hierarchical clustering algorithm is used. The code of BFC is obtained from a link in [46]. As BFC involves the Cholesky factorization of the covariance matrices of data and the covariance matrices of some data are not positive definite, BFC may not be applicable to some datasets. The codes of FSC and MEC are obtained from Github⁸. The codes of KFCM and 2PFCM are shared by the authors of [47] and [54], respectively. The Euclidean distance is used as the dissimilarity measure in all algorithms.

The performance evaluation for the experimental results is based on nineteen internal criteria listed in Table 3 in [26] and three external criteria described in subsection 4.1 in [26]. Due to the wide range of values of WGSS, CHI, XBI, and TWI, they are normalized by p , $(n - k)/(k - 1)$, n , and pk , respectively, to facilitate the later tabular presentation.

Tables II-V tabulate the means and standard deviations of the internal and external cluster validity indices values over 50

²https://www.mathworks.com/help/stats/kmeans.html?s_tid=srchtitle_kmean_1

³<https://github.com/xuyxu/Clustering>

⁴<https://github.com/DebolinaPaul/EWP>

⁵<https://www.mathworks.com/help/stats/spectralcluster.html>

⁶https://www.mathworks.com/help/stats/hierarchical-clustering.html?s_tid=srchtitle_hierarchical_%20clustering_1

⁷<https://www.mathworks.com/help/fuzzy/fcm.html>

⁸https://github.com/kailugaji/Fuzzy_Clustering_Algorithms

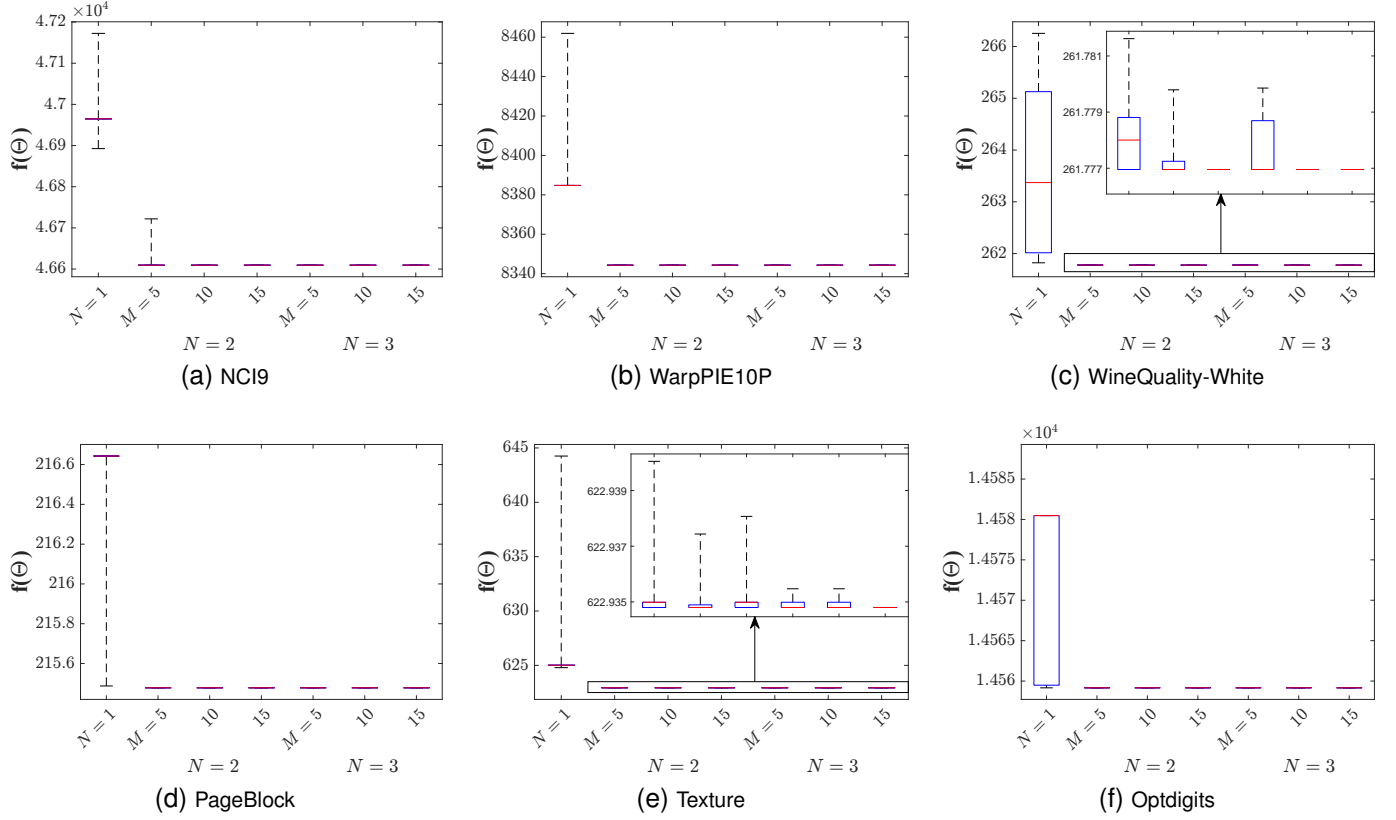


Fig. 4. Monte Carlo test results using CAFCA with several values of N and M on the six datasets.

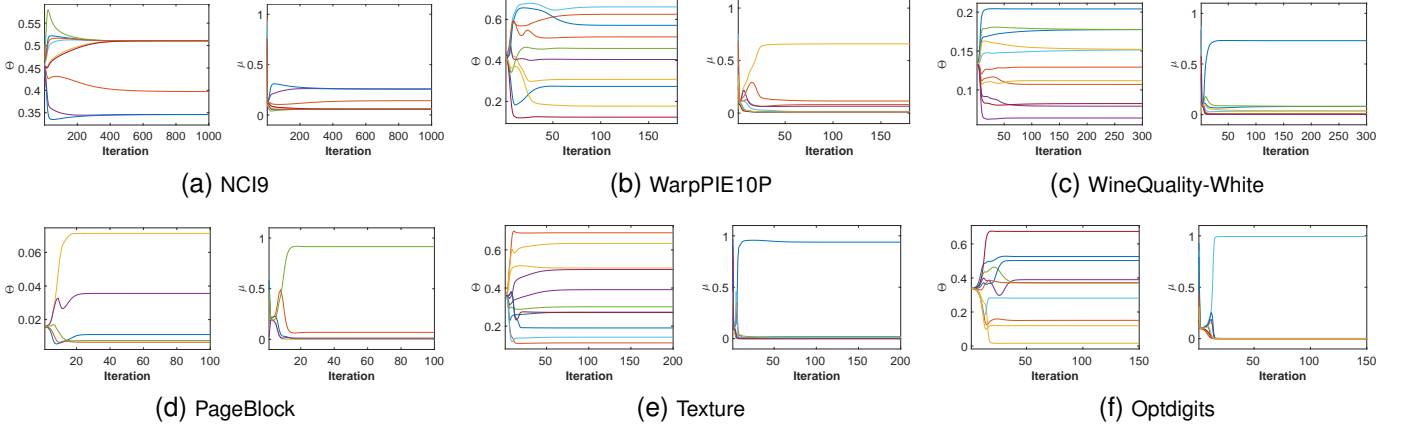


Fig. 5. Snapshots of the convergent centers Θ and the membership degrees μ values in the FCM clustering loop of CAFCM (Steps 6-10) on the six datasets, where the lines in the left subplots portray the first feature values of k centers, and the lines in the right subplots portray the k membership degrees.

runs by using CAFCM and thirteen prevailing algorithms with random initialization on the eight datasets, where \times indicates “not applicable”, and the best and second-best results are boldfaced and underlined, respectively. Specifically, CAFCM achieves 81 best and 20 second-best means out of 168 entries (i.e., 48.21% and 60.12% for the best and the best plus the second-best), and CAPKM++2.0 ranks in second place, achieving 40 best and 55 second-best means (i.e., 23.81% and 56.55%), and SC ranks in third place, achieving 23 best and 3 second-best means (i.e., 13.69% and 15.48%). Fig. 8 depicts the counts of the best and best plus second-best index mean values by using CAFCM and the thirteen baselines. As shown in Fig. 8, CAFCM, CAPKM++2.0, and SC rank in

the first three places in terms of the counts of the best index mean values. CAFCM, CAPKM++2.0, and PKM rank in the first three places in terms of the counts of best plus second-best index mean values. In addition, the standard deviations of the results using CAFCM are zero, indicating the highest consistency of the algorithm.

E. Complexity Analysis

As shown in Table I and Table S-II in the supplementary materials, the suitable number of modules N is 2 or 3, for 18 datasets with various values of n , p , and k . As N is a small constant, the spatial complexity of CAFCM is the same as FCM (i.e., $O((n+p)k)$ [66]).

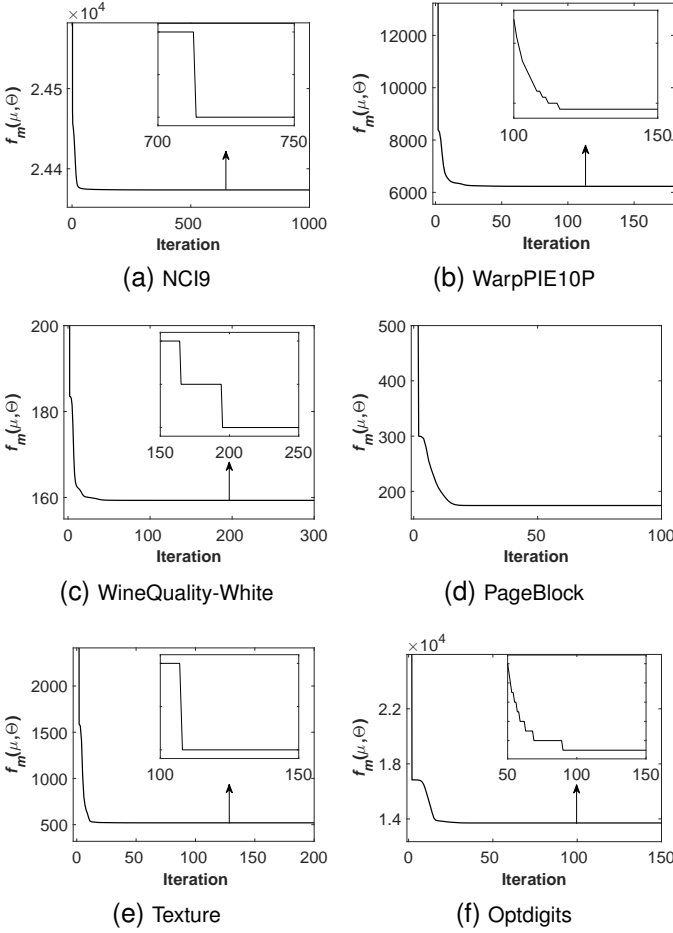


Fig. 6. Snapshots of the fuzzy objective function values of $f_m(\mu, \Theta)$ in (2) with $m = 1.5$ in the FCM clustering loop of CAFCM (Steps 6-10) on the six datasets.

The time complexity is empirically estimated via non-negative least-squares regression using the numbers of iterations on the 18 datasets:

$$\begin{aligned} \min_w & \|Cw - T\|_2^2, \\ \text{s.t. } & w \geq 0, \end{aligned}$$

where $w \in \mathbb{R}^{38}$ is the weight vector of the terms, $T \in \mathbb{R}^{18}$ is the vector of iteration counts, and $C \in \mathbb{R}^{18 \times 38}$ is the matrix of 38 combinations of polynomials and logarithms of n , m , and p . Table S-VIII in the supplementary materials lists the 38 combinations of polynomials and logarithms of n , m , and p , and their estimated coefficients. By neglecting the terms with their coefficients w smaller than 0.0001, the resulting estimate is $2,288,239k^2np + 351,783k^2np \log(p)$. As the second term is of higher order, the estimated time complexity of CAFCM is $O(k^2np \log(p))$. As the time complexity of FCM is $O(k^2np)$ per iteration [66], it is $\log(p)$ times that of FCM.

V. CONCLUDING REMARKS

In this paper, a collaborative annealing fuzzy c -means clustering algorithm is proposed. The experimental results on eight datasets demonstrate that the proposed algorithm with only two or three modules statistically outperforms thirteen

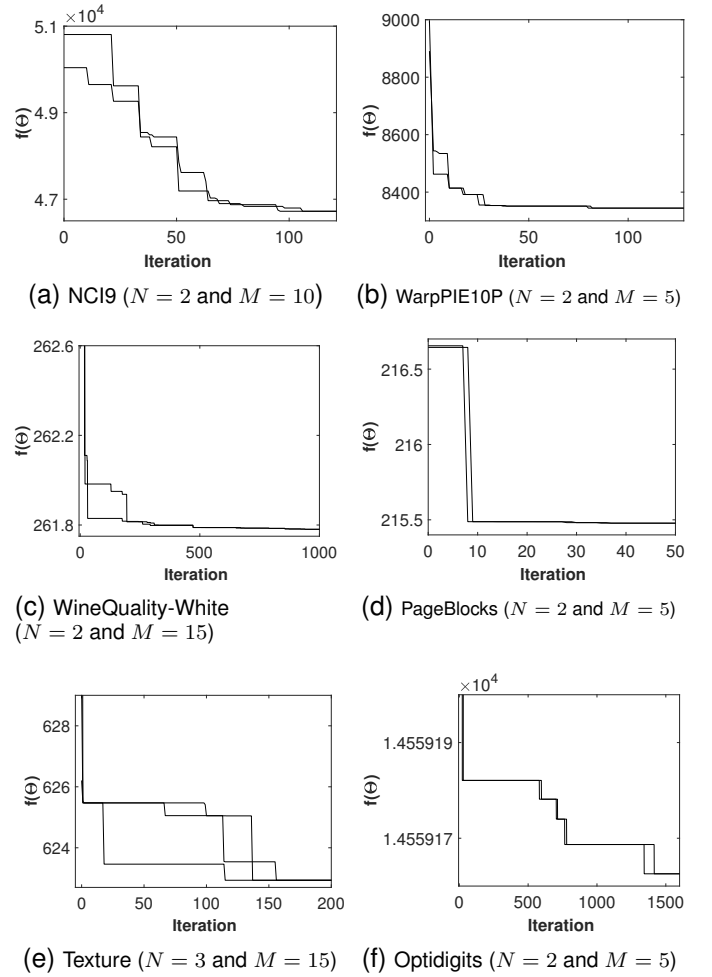


Fig. 7. The descending objective function values of $f(\Theta)$ in the annealing loop of CAFCM (Steps 2-33) on the six datasets.

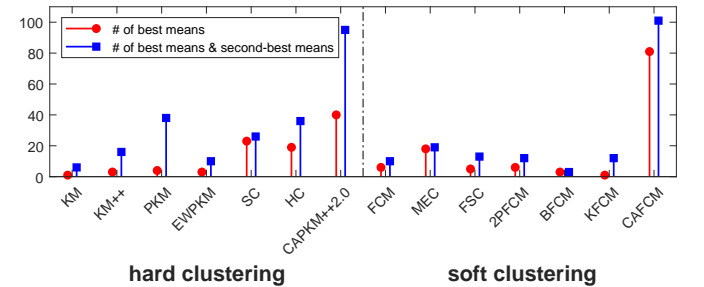


Fig. 8. The counts of the best and best plus second-best index mean values using CAFCM and the thirteen baselines.

competing algorithms in terms of many cluster validity indices. The proposed method achieves superior performance, owing to the adoption of the annealing procedure to phase out fuzziness, as well as collaborative modules to maximize clustering quality and eliminate the influence of initial solutions on clustering performance. Further research may include improving the efficiency of the proposed method, extending it for robust clustering to cluster data in the presence of noises or outliers, extending it for semi-supervised clustering to leverage information from labeled and unlabeled data, extending it for multi-view clustering to take into account of multiple

perspectives or representations of data, and applying it to specific problems in science and engineering.

TABLE II

THE MEAN VALUES AND STANDARD DEVIATIONS OF INTERNAL AND EXTERNAL CLUSTER VALIDITY INDICES RESULTING FROM CAFCM, AND THIRTEEN BASELINES ON NCI9 AND WARPPIE10P, WHERE $N = 2$ AND $M = 10$ IN CAPKM++2.0 AND CAFCM ON NCI9, AND $N = 2$ AND $M = 5$ IN CAPKM++2.0 AND CAFCM ON WARPPIE10P.

NCI9	KM	KM++	PKM	EWPKM	SC	HC	CAPKM++2.0
WGSS↓	5.2462 ± 0.1468	5.2877 ± 0.1555	4.8592 ± 0.0129	4.8614 ± 0.0114	6.5683 ± 0.1529	5.0366 ± 0.0000	4.8116 ± 0.0029
MRI↓	0.8730 ± 0.0147	0.8734 ± 0.0135	0.8468 ± 0.0056	0.8472 ± 0.0052	1.0039 ± 0.0117	0.8442 ± 0.0000	0.8335 ± 0.0012
GPI↓	0.0488 ± 0.0138	0.0515 ± 0.0149	0.0246 ± 0.0025	0.0247 ± 0.0023	0.2306 ± 0.0263	0.0247 ± 0.0000	0.0183 ± 0.0008
BHGI↑	0.6390 ± 0.0780	0.6386 ± 0.0726	0.7392 ± 0.0340	0.7364 ± 0.0318	-0.0209 ± 0.0584	0.7685 ± 0.0000	0.8268 ± 0.0067
CI↓	0.1656 ± 0.0342	0.1641 ± 0.0319	0.1234 ± 0.0142	0.1246 ± 0.0133	0.5009 ± 0.0347	0.1102 ± 0.0000	0.0866 ± 0.0028
TI↑	0.3300 ± 0.0412	0.3383 ± 0.0420	0.3217 ± 0.0200	0.3195 ± 0.0189	-0.0142 ± 0.0397	0.3551 ± 0.0000	0.3802 ± 0.0040
DGI↑	1.4203 ± 0.0616	1.4370 ± 0.0812	1.5220 ± 0.0197	1.5147 ± 0.0191	1.2395 ± 0.0984	1.5442 ± 0.0000	1.4940 ± 0.0216
RLI↑	0.1864 ± 0.0046	0.1883 ± 0.0059	0.1936 ± 0.0006	0.1935 ± 0.0005	0.1218 ± 0.0048	0.1949 ± 0.0000	0.1954 ± 0.0002
CHI↑	0.4874 ± 0.0341	0.5000 ± 0.0418	0.5550 ± 0.0041	0.5543 ± 0.0036	0.1548 ± 0.0140	0.5531 ± 0.0000	0.5704 ± 0.0009
RTI↓	2.1592 ± 0.4266	2.1165 ± 0.5580	1.8350 ± 0.0743	1.8238 ± 0.0725	6.6390 ± 2.6748	1.8860 ± 0.0000	1.4976 ± 0.0811
WGI↑	0.1928 ± 0.0142	0.1938 ± 0.0175	0.2093 ± 0.0047	0.2088 ± 0.0047	0.1237 ± 0.0325	0.2143 ± 0.0000	0.2347 ± 0.0027
DI↑	0.6114 ± 0.0332	0.6227 ± 0.0336	0.6634 ± 0.0089	0.6626 ± 0.0113	0.4727 ± 0.0127	0.6890 ± 0.0000	0.6568 ± 0.0075
BHI↑	718.3157 ± 59.4908	727.5179 ± 55.6430	777.2263 ± 5.3801	778.3961 ± 5.3559	520.9616 ± 150.5932	705.6937 ± 0.0000	760.8223 ± 6.2293
PBMI↑	44.2921 ± 8.8454	47.9437 ± 11.1767	57.0968 ± 2.6056	57.2552 ± 2.3421	48.1918 ± 12.6702	52.3096 ± 0.0000	41.1212 ± 0.1705
XBI↓	0.0120 ± 0.0010	0.0119 ± 0.0011	0.0102 ± 0.0000	0.0102 ± 0.0000	0.0161 ± 0.0006	0.0102 ± 0.0000	0.0101 ± 0.0000
DBI↓	2.3937 ± 0.1579	2.3963 ± 0.1722	2.5070 ± 0.0599	2.5108 ± 0.0578	2.6560 ± 0.5068	2.2793 ± 0.0000	2.2491 ± 0.0248
LSSRI↑	-0.7765 ± 0.0666	-0.8055 ± 0.0865	-0.5888 ± 0.0074	-0.5900 ± 0.0066	-1.8693 ± 0.0870	-0.5921 ± 0.0000	-0.5615 ± 0.0017
TWI↓	0.5749 ± 0.0120	0.5800 ± 0.0154	0.5399 ± 0.0014	0.5401 ± 0.0013	0.7271 ± 0.0087	0.5406 ± 0.0000	<u>0.5346 ± 0.0003</u>
ACC↑	0.3973 ± 0.0417	0.3907 ± 0.0464	0.4373 ± 0.0141	0.4317 ± 0.0144	0.2623 ± 0.0225	0.4667 ± 0.0000	0.4640 ± 0.0085
NMI↑	0.3976 ± 0.0440	0.3922 ± 0.0447	0.4753 ± 0.0134	0.4720 ± 0.0140	0.2475 ± 0.0302	0.4750 ± 0.0000	0.4811 ± 0.0056
ARI↑	0.1113 ± 0.0412	0.1084 ± 0.0453	0.1773 ± 0.0138	0.1729 ± 0.0147	0.0019 ± 0.0164	0.1946 ± 0.0000	0.2005 ± 0.0082
NCI9	FCM	MEC	FSC	2PFCM	BFC	KFCM	CAFCM
WGSS↓	6.4080 ± 0.0000	6.4080 ± 0.0000	6.3000 ± 0.1441	6.4080 ± 0.0000	×	6.2337 ± 0.1136	4.7992 ± 0.0000
MRI↓	0.8775 ± 0.0000	0.8775 ± 0.0000	0.9983 ± 0.0087	0.8775 ± 0.0000	×	0.8862 ± 0.0035	0.8314 ± 0.0000
GPI↓	0.0872 ± 0.0000	0.0872 ± 0.0000	0.0971 ± 0.0058	0.0872 ± 0.0000	×	0.0988 ± 0.0062	0.0168 ± 0.0000
BHGI↑	0.6512 ± 0.0000	0.6512 ± 0.0000	0.0052 ± 0.0433	0.6512 ± 0.0000	×	0.5948 ± 0.0226	0.8553 ± 0.0000
CI↓	0.1481 ± 0.0000	0.1481 ± 0.0000	0.4534 ± 0.0187	0.1481 ± 0.0000	×	0.1732 ± 0.0101	0.0750 ± 0.0000
TI↑	0.4606 ± 0.0000	0.4606 ± 0.0000	0.0023 ± 0.0193	0.4606 ± 0.0000	×	0.4152 ± 0.0153	0.4128 ± 0.0000
DGI↑	1.5162 ± 0.0000	1.5162 ± 0.0000	1.2437 ± 0.0333	1.5162 ± 0.0000	×	1.4460 ± 0.0692	1.4970 ± 0.0000
RLI↑	0.2620 ± 0.0000	0.2620 ± 0.0000	0.1231 ± 0.0052	0.2620 ± 0.0000	×	0.1976 ± 0.0110	0.1970 ± 0.0000
CHI↑	1.6299 ± 0.0000	1.6299 ± 0.0000	0.1587 ± 0.0172	1.6299 ± 0.0000	×	0.5960 ± 0.0971	0.5744 ± 0.0000
RTI↓	1.3893 ± 0.0000	1.3893 ± 0.0000	4.9573 ± 0.5891	1.3893 ± 0.0000	×	1.5432 ± 0.3750	1.7243 ± 0.0000
WGI↑	0.2265 ± 0.0000	0.2265 ± 0.0000	0.0609 ± 0.0058	0.2265 ± 0.0000	×	0.2348 ± 0.0316	0.2366 ± 0.0000
DI↑	0.5961 ± 0.0000	0.5961 ± 0.0000	0.4831 ± 0.0153	0.5961 ± 0.0000	×	0.5718 ± 0.0303	0.7067 ± 0.0000
BHI↑	1031.1357 ± 0.0000	1031.1357 ± 0.0000	1025.6173 ± 26.0115	1031.1357 ± 0.0000	×	588.0926 ± 152.9647	695.6437 ± 0.0000
PBMI↑	220.2380 ± 0.0000	220.2380 ± 0.0000	12.7660 ± 3.7023	220.2380 ± 0.0000	×	90.7854 ± 22.4696	46.3868 ± 0.0000
XBI↓	0.0131 ± 0.0000	0.0131 ± 0.0000	0.0163 ± 0.0003	0.0131 ± 0.0000	×	0.0136 ± 0.0013	0.0101 ± 0.0000
DBI↓	2.3399 ± 0.0000	2.3399 ± 0.0000	3.9249 ± 0.1331	2.3399 ± 0.0000	×	1.8879 ± 0.3532	2.1064 ± 0.0000
LSSRI↑	-1.7195 ± 0.0000	-1.7195 ± 0.0000	-1.8462 ± 0.1079	-1.7195 ± 0.0000	×	-1.4070 ± 0.0860	-0.5543 ± 0.0000
TWI↓	0.7120 ± 0.0000	0.7120 ± 0.0000	0.7247 ± 0.0107	0.7120 ± 0.0000	×	0.6741 ± 0.0115	0.5332 ± 0.0000
ACC↑	0.2000 ± 0.0000	0.2000 ± 0.0000	0.2960 ± 0.0253	0.2000 ± 0.0000	×	0.2377 ± 0.0146	0.4667 ± 0.0000
NMI↑	0.0649 ± 0.0000	0.0649 ± 0.0000	0.2855 ± 0.0335	0.0649 ± 0.0000	×	0.1473 ± 0.0197	0.4553 ± 0.0000
ARI↑	0.0050 ± 0.0000	0.0050 ± 0.0000	0.0007 ± 0.0247	0.0050 ± 0.0000	×	0.0107 ± 0.0055	0.1775 ± 0.0000
WarpPIE10P	KM	KM++	PKM	EWPKM	SC	HC	CAPKM++2.0
WGSS↓	3.6702 ± 0.1250	3.6396 ± 0.1102	3.4673 ± 0.0081	3.4660 ± 0.0053	5.4244 ± 0.1375	3.5330 ± 0.0000	3.4485 ± 0.0007
MRI↓	0.5617 ± 0.0153	0.5549 ± 0.0114	0.5519 ± 0.0020	0.5528 ± 0.0011	1.0070 ± 0.0072	0.5548 ± 0.0000	0.5375 ± 0.0014
GPI↓	0.0184 ± 0.0038	0.0168 ± 0.0025	0.0152 ± 0.0003	0.0154 ± 0.0001	0.2305 ± 0.0077	0.0168 ± 0.0000	0.0132 ± 0.0002
BHGI↑	0.8269 ± 0.0287	0.8398 ± 0.0231	0.8334 ± 0.0030	0.8314 ± 0.0021	-0.0002 ± 0.0140	0.8260 ± 0.0000	0.8589 ± 0.0012
CI↓	0.0924 ± 0.0127	0.0867 ± 0.0113	0.0938 ± 0.0014	0.0945 ± 0.0012	0.4955 ± 0.0101	0.0925 ± 0.0000	0.0793 ± 0.0008
TI↑	0.3804 ± 0.0204	0.3849 ± 0.0232	0.3555 ± 0.0005	0.3550 ± 0.0015	-0.0002 ± 0.0097	0.3630 ± 0.0000	0.3715 ± 0.0009
DGI↑	0.4522 ± 0.0789	0.4596 ± 0.0865	0.4318 ± 0.0280	0.4442 ± 0.0285	0.6521 ± 0.0102	0.6178 ± 0.0000	0.6017 ± 0.0483
RLI↑	0.2544 ± 0.0030	0.2548 ± 0.0019	0.2575 ± 0.0002	0.2575 ± 0.0001	0.1493 ± 0.0052	0.2550 ± 0.0000	0.2576 ± 0.0002
CHI↑	2.0035 ± 0.1020	2.0236 ± 0.0852	2.1704 ± 0.0073	2.1717 ± 0.0048	0.3086 ± 0.0273	2.0299 ± 0.0000	2.1877 ± 0.0006
RTI↓	1.1935 ± 0.3724	1.0997 ± 0.1915	0.9863 ± 0.0381	0.9807 ± 0.0281	3.2132 ± 0.6500	0.9082 ± 0.0000	0.9109 ± 0.0115
WGI↑	0.3000 ± 0.0166	0.3023 ± 0.0167	0.3032 ± 0.0016	0.3035 ± 0.0013	0.1608 ± 0.0138	0.3058 ± 0.0000	0.3275 ± 0.0046
DI↑	0.1508 ± 0.0278	0.1571 ± 0.0299	0.1619 ± 0.0106	0.1662 ± 0.0079	0.1653 ± 0.0000	0.2062 ± 0.0000	0.2284 ± 0.0188
BHI↑	41.1859 ± 1.4855	41.8175 ± 1.4292	39.6807 ± 0.5807	39.4854 ± 0.3599	29.1643 ± 1.4002	42.0479 ± 0.0000	41.2249 ± 0.0376
PBMI↑	14.8197 ± 1.7981	15.7846 ± 1.8157	15.4603 ± 0.1819	15.2328 ± 0.0447	7.4846 ± 0.2832	15.1854 ± 0.0000	15.2649 ± 0.1076
XBI↓	0.0322 ± 0.0136	0.0311 ± 0.0116	0.0301 ± 0.0061	0.0281 ± 0.0020	0.0161 ± 0.0004	0.0146 ± 0.0000	0.0156 ± 0.0036
DBI↓	1.6531 ± 0.0813	1.6543 ± 0.0833	1.5892 ± 0.0337	1.5787 ± 0.0106	1.6824 ± 0.0650	<u>1.5338 ± 0.0000</u>	1.5912 ± 0.0216
LSSRI↑	0.6911 ± 0.0509	0.7040 ± 0.0432	0.7749 ± 0.0034	0.7755 ± 0.0022	-1.1803 ± 0.1009	0.7080 ± 0.0000	0.7829 ± 0.0003
TWI↓	0.3670 ± 0.0125	0.3639 ± 0.0106	0.3467 ± 0.0008	0.3466 ± 0.0005	0.8404 ± 0.0185	0.3628 ± 0.0000	<u>0.3448 ± 0.0001</u>
ACC↑	0.2808 ± 0.0238	0.2849 ± 0.0223	0.2726 ± 0.0043	0.2720 ± 0.0042	0.2874 ± 0.0136	0.2857 ± 0.0000	0.2827 ± 0.0037
NMI↑	0.3006 ± 0.0334	0.3024 ± 0.0304	0.3062 ± 0.0037	0.3140 ± 0.0054	0.3835 ± 0.0155	0.3614 ± 0.0000	0.3112 ± 0.0051
ARI↑	0.0872 ± 0.0209	0.0893 ± 0.0204	0.0927 ± 0.0040	0.0962 ± 0.0044	0.0917 ± 0.0162	0.1117 ± 0.0000	0.0932 ± 0.0017
WarpPIE10P	FCM	MEC	FSC	2PFCM	BFC	KFCM	CAFCM
WGSS↓	4.0995 ± 0.0781	5.7692 ± 0.4605	4.5079 ± 0.2281	4.1417 ± 0.0000	×	4.9026 ± 0.3384	3.4481 ± 0.0000
MRI↓	0.5964 ± 0.0033	0.6727 ± 0.0235	0.6437 ± 0.0320	0.5966 ± 0.0000	×	0.6351 ± 0.0209	0.5368 ± 0.0000
GPI↓	0.0265 ± 0.0012	0.0730 ± 0.0137	0.0457 ± 0.0130	0.0267 ± 0.0000	×	0.0506 ± 0.0119	0.0131 ± 0.0000
BHGI↑	0.7720 ± 0.0045	0.6944 ± 0.0510	0.6857 ± 0.0667	0.7723 ± 0.0000	×	0.7501 ± 0.0406	0.8594 ± 0.0000
CI↓	0.1181 ± 0.0020	0.1350 ± 0.0258	0.1488 ± 0.0297	0.1176 ± 0.0000	×	0.1118 ± 0.0185	0.0788 ± 0.0000
TI↑	0.3719 ± 0.0054	0.4790 ± 0.0341	0.3676 ± 0.0401	0.3739 ± 0.0000	×	0.4743 ± 0.0371	0.3712 ± 0.0000
DGI↑	0.3726 ± 0.0150	0.4923 ± 0.1518	0.3584 ± 0.0614	0.3753 ± 0.0000	×	0.4407 ± 0.0981	0.6128 ± 0.0000
RLI↑	0.2672 ± 0.0069	0.3029 ± 0.0253	0.2321 ± 0.0095	0.2737 ± 0.0000	×	0.2742 ± 0.0215	0.2575 ± 0.0000
CHI↑	1.9728 ± 0.1043	2.0753 ± 0.4907	1.2087 ± 0.1801	2.0772 ± 0.0000	×	1.7966 ± 0.3492	2.1881 ± 0.0000
RTI↓	1.8281 ± 0.1085	1.1546 ± 0.6850	2.9239 ± 1.1012	1.8725 ± 0.0000	×	2.2566 ± 1.4066	0.9166 ± 0.0000
WGI↑	0.2094 ± 0.0058	0.2998 ± 0.0599	0.1626 ± 0.0444	0.2108 ± 0.0000	×	0.2580 ± 0.0438	0.3298 ± 0.0000
DI↑	0.1200 ± 0.0055	0.1152 ± 0.0347	0.1021 ± 0.0166	0.1216 ± 0.0000	×	0.1179 ± 0.0261	0.2357 ± 0.0000
BHI↑	47.7023 ± 1.7305	56.2621 ± 8.4753	56.0150 ± 5.3085	49.0781 ± 0.0000	×	44.7456 ± 6.3442	41.2083 ± 0.0000
PBMI↑	18.3786 ± 1.6131	35.9067 ± 10.626	18.6801 ± 1.8138	18.6328 ± 0.0000	×	15.8542 ± 4.2921	15.2014 ± 0.0000
XBI↓	0.0454 ± 0.0056	0.0478 ± 0.0260	0.0513 ± 0.0168	0.0446 ± 0.0000	×	0.0459 ± 0.0199	0.0143 ± 0.0000
DBI↓	2.0949 ± 0.0706	1.4158 ± 0.2782	2.4521 ± 0.2813	2.1304 ± 0.0000	×	1.6098 ± 0.3075	1.6021 ± 0.0000
LSSRI↑	0.4750 ± 0.0242	-0.3174 ± 0.2081	0.1485 ± 0.1483	0.4698 ± 0.0000	×	0.0836 ± 0.1595	0.7830 ± 0.0000
TWI↓	0.4215 ± 0.0063	0.6353 ± 0.0555	0.5091 ± 0.0404	0.4229 ± 0.0000	×	0.5268 ± 0.0434	0.3448 ± 0.0000
ACC↑	0.1991 ± 0.0045	0.1373 ± 0.0164	0.2636 ± 0.0281	0.2000 ± 0.0000	×	0.1675 ± 0.0196	0.2810 ± 0.0000
NMI↑	0.1378 ± 0.0103	0.0587 ± 0.0249	0.2673 ±				

TABLE III

THE MEAN VALUES AND STANDARD DEVIATIONS OF INTERNAL AND EXTERNAL CLUSTER VALIDITY INDICES RESULTING FROM CAFCM, AND THIRTEEN BASELINES ON WQ-WHITE AND PAGEBLOCKS, WHERE $N = 2$ AND $M = 15$ IN CAPKM++2.0 AND CAFCM ON WQ-WHITE, AND $N = 2$ AND $M = 5$ IN CAPKM++2.0 AND CAFCM ON PAGEBLOCKS.

WQ-White	KM	KM++	PKM	EWPKM	SC	HC	CAPKM++2.0
WGSS↓	24.1112 ± 0.2265	24.0518 ± 0.2140	24.1402 ± 0.0557	31.1401 ± 0.5426	26.7792 ± 0.5784	24.7211 ± 0.0000	23.7983 ± 0.0003
MRI↓	0.6234 ± 0.0049	0.6210 ± 0.0041	0.6218 ± 0.0023	0.7862 ± 0.0086	0.6990 ± 0.0118	0.6672 ± 0.0000	0.6134 ± 0.0003
GPI↓	0.0268 ± 0.0011	0.0266 ± 0.0010	0.0261 ± 0.0004	0.0568 ± 0.0010	0.0684 ± 0.0094	0.0409 ± 0.0000	0.0259 ± 0.0001
BHGI↑	0.7087 ± 0.0111	0.7137 ± 0.0095	0.7091 ± 0.0044	0.3820 ± 0.0164	0.5778 ± 0.0217	0.6272 ± 0.0000	0.7315 ± 0.0007
CI↓	0.1318 ± 0.0048	0.1295 ± 0.0041	0.1314 ± 0.0019	0.2658 ± 0.0070	0.1825 ± 0.0103	0.1638 ± 0.0000	0.1218 ± 0.0003
TI↑	0.3042 ± 0.0100	0.3077 ± 0.0090	0.3002 ± 0.0021	0.1639 ± 0.0082	0.3277 ± 0.0061	0.2939 ± 0.0000	0.3213 ± 0.0003
DGI↑	0.0985 ± 0.0304	0.0925 ± 0.0236	0.0857 ± 0.0294	0.0788 ± 0.0117	0.0724 ± 0.0287	0.3741 ± 0.0000	0.0897 ± 0.0177
RLI↑	0.1982 ± 0.0045	0.1991 ± 0.0040	0.1936 ± 0.0005	0.1918 ± 0.0043	0.1873 ± 0.0032	0.1921 ± 0.0000	0.2020 ± 0.0001
CHI↑	1.2958 ± 0.0215	1.3019 ± 0.0189	1.2927 ± 0.0054	0.5167 ± 0.0211	0.9218 ± 0.0532	1.0443 ± 0.0000	1.3258 ± 0.0000
RTI↓	1.2338 ± 0.1081	1.2356 ± 0.1258	1.2730 ± 0.0420	4.6374 ± 0.6606	1.7116 ± 0.6944	1.4968 ± 0.0000	1.0232 ± 0.0355
WGI↑	0.2339 ± 0.0061	0.2358 ± 0.0052	0.2313 ± 0.0012	0.0372 ± 0.0044	0.2095 ± 0.0123	0.1669 ± 0.0000	0.2432 ± 0.0001
DI↑	0.0107 ± 0.0032	0.0105 ± 0.0027	0.0101 ± 0.0029	0.0105 ± 0.0015	0.0079 ± 0.0031	0.0389 ± 0.0000	0.0108 ± 0.0021
BHI↑	0.0580 ± 0.0017	0.0581 ± 0.0010	0.0577 ± 0.0004	0.0822 ± 0.0007	0.0501 ± 0.0017	0.0642 ± 0.0000	0.0593 ± 0.0001
PBMI↑	0.0090 ± 0.0008	0.0097 ± 0.0051	0.0088 ± 0.0003	0.0043 ± 0.0001	0.0187 ± 0.0005	0.0077 ± 0.0000	0.0089 ± 0.0000
XBI↓	0.0441 ± 0.0538	0.0411 ± 0.0283	0.0601 ± 0.0726	0.0662 ± 0.0277	0.1812 ± 0.4440	0.0022 ± 0.0000	0.0385 ± 0.0076
DBI↓	1.7215 ± 0.0582	1.7092 ± 0.0605	1.7443 ± 0.0134	3.3640 ± 0.2439	1.5007 ± 0.0831	1.8248 ± 0.0000	1.6309 ± 0.0040
LSSRI↑	0.2590 ± 0.0166	0.2637 ± 0.0146	0.2567 ± 0.0042	-0.6611 ± 0.0406	-0.0832 ± 0.0609	0.0433 ± 0.0000	0.2820 ± 0.0000
TWI↓	2.1919 ± 0.0206	2.1860 ± 0.0181	2.1947 ± 0.0052	3.3182 ± 0.0459	2.6203 ± 0.0762	2.4613 ± 0.0000	2.1635 ± 0.0000
ACC↑	0.1911 ± 0.0110	0.1943 ± 0.0110	0.1883 ± 0.0028	0.1778 ± 0.0082	0.3136 ± 0.0223	0.2201 ± 0.0000	0.2034 ± 0.0009
NMI↑	0.0828 ± 0.0026	0.0825 ± 0.0022	0.0833 ± 0.0012	0.0531 ± 0.0045	0.0762 ± 0.0042	0.0695 ± 0.0000	0.0809 ± 0.0004
ARI↑	0.0314 ± 0.0014	0.0315 ± 0.0014	0.0314 ± 0.0007	0.0173 ± 0.0018	0.0411 ± 0.0038	0.0315 ± 0.0000	0.0314 ± 0.0002
WQ-White	FCM	MEC	FSC	2PFCM	BFC	KFCM	CAFCM
WGSS↓	30.3011 ± 0.2196	30.5183 ± 1.0614	34.1901 ± 0.8792	30.5788 ± 0.0000	39.0307 ± 0.8555	29.1012 ± 0.9733	23.7979 ± 0.0000
MRI↓	0.7324 ± 0.0012	0.7389 ± 0.0080	0.9225 ± 0.0082	0.7323 ± 0.0000	0.9606 ± 0.0060	0.7322 ± 0.0125	0.6130 ± 0.0000
GPI↓	0.0651 ± 0.0031	0.1110 ± 0.0097	0.0857 ± 0.0044	0.0661 ± 0.0000	0.0773 ± 0.0011	0.0954 ± 0.0121	0.0258 ± 0.0000
BHGI↑	0.5026 ± 0.0019	0.5192 ± 0.0151	1.1354 ± 0.0146	0.5032 ± 0.0000	0.0703 ± 0.0113	0.5217 ± 0.0268	0.7323 ± 0.0000
CI↓	0.2174 ± 0.0009	0.2180 ± 0.0087	0.3760 ± 0.0068	0.2171 ± 0.0000	0.4016 ± 0.0047	0.2114 ± 0.0127	0.1215 ± 0.0000
TI↑	0.2570 ± 0.0064	0.3524 ± 0.0166	0.0603 ± 0.0063	0.2597 ± 0.0000	0.0287 ± 0.0046	0.3291 ± 0.0264	0.3216 ± 0.0000
DGI↑	0.0447 ± 0.0271	0.0844 ± 0.0662	0.0476 ± 0.0099	0.0565 ± 0.0000	0.0000 ± 0.0000	0.0914 ± 0.0583	0.1489 ± 0.0000
RLI↑	0.1589 ± 0.0023	0.1589 ± 0.0109	0.1106 ± 0.0077	0.1658 ± 0.0000	0.0660 ± 0.0049	0.1616 ± 0.0071	0.2019 ± 0.0000
CHI↑	0.6882 ± 0.0227	0.6668 ± 0.1235	0.1728 ± 0.0301	0.7568 ± 0.0000	0.0724 ± 0.0118	0.7021 ± 0.0790	1.3258 ± 0.0000
RTI↓	28.4805 ± 11.1635	6.2702 ± 4.4866	61.0821 ± 18.5534	31.9810 ± 0.0000	303.0457 ± 124.7866	3.4390 ± 1.3883	1.0290 ± 0.0000
WGI↑	0.0526 ± 0.0040	0.0678 ± 0.0339	0.0069 ± 0.0041	0.0602 ± 0.0000	0.0005 ± 0.0020	0.0838 ± 0.0228	0.2430 ± 0.0000
DI↑	0.0046 ± 0.0027	0.0089 ± 0.0070	0.0067 ± 0.0014	0.0066 ± 0.0000	0.0000 ± 0.0000	0.0100 ± 0.0064	0.0179 ± 0.0000
BHI↑	0.0698 ± 0.0036	0.0561 ± 0.0065	0.1028 ± 0.0043	0.0757 ± 0.0000	0.1159 ± 0.0014	0.0590 ± 0.0054	0.0593 ± 0.0000
PBMI↑	0.0055 ± 0.0004	0.0056 ± 0.0026	0.0026 ± 0.0006	0.0065 ± 0.0000	0.0007 ± 0.0002	0.0037 ± 0.0014	0.0089 ± 0.0000
XBI↓	0.5431 ± 0.7058	0.7697 ± 1.0280	0.1935 ± 0.0874	0.0947 ± 0.0000	∞ ± NaN	0.2875 ± 0.5703	0.0131 ± 0.0000
DBI↓	5.9397 ± 0.6268	2.3661 ± 0.3880	9.5955 ± 0.9188	5.8677 ± 0.0000	22.1934 ± 3.0747	2.2232 ± 0.1841	1.6294 ± 0.0000
LSSRI↑	-0.3826 ± 0.0090	-0.6364 ± 0.1396	-1.7714 ± 0.1821	-0.3843 ± 0.0000	-2.6392 ± 0.1691	-0.4159 ± 0.1070	0.2820 ± 0.0000
TWI↓	2.9913 ± 0.0109	3.2871 ± 0.1599	4.2932 ± 0.1104	2.9934 ± 0.0000	4.6927 ± 0.0516	3.0302 ± 0.1278	2.1634 ± 0.0000
ACC↑	0.2750 ± 0.0082	0.4071 ± 0.0319	0.1794 ± 0.0078	0.2799 ± 0.0000	0.1216 ± 0.0034	0.3585 ± 0.0366	0.2023 ± 0.0000
NMI↑	0.0791 ± 0.0006	0.0843 ± 0.0064	0.0302 ± 0.0036	0.0796 ± 0.0000	0.0144 ± 0.0016	0.0789 ± 0.0053	0.0806 ± 0.0000
ARI↑	0.0452 ± 0.0023	0.0697 ± 0.0108	0.0098 ± 0.0016	0.0464 ± 0.0000	0.0042 ± 0.0008	0.0597 ± 0.0136	0.0311 ± 0.0000
PageBlocks	KM	KM++	PKM	EWPKM	SC	HC	CAPKM++2.0
WGSS↓	21.7169 ± 0.3282	22.1370 ± 0.6964	21.6463 ± 0.0431	38.1295 ± 0.0053	24.9753 ± 0.0000	22.5422 ± 0.0000	21.5478 ± 0.0000
MRI↓	0.4072 ± 0.0058	0.4087 ± 0.0072	0.4080 ± 0.0046	0.5264 ± 0.0001	0.4738 ± 0.0000	0.4167 ± 0.0000	0.3974 ± 0.0001
GPI↓	0.0504 ± 0.0019	0.0517 ± 0.0033	0.0504 ± 0.0012	0.0892 ± 0.0001	0.0797 ± 0.0000	0.0547 ± 0.0000	0.0476 ± 0.0000
BHGI↑	0.7577 ± 0.0172	0.7617 ± 0.0154	0.7533 ± 0.0144	0.6198 ± 0.0003	0.6547 ± 0.0000	0.7583 ± 0.0000	0.7867 ± 0.0002
CI↓	0.0840 ± 0.0055	0.0840 ± 0.0055	0.0852 ± 0.0046	0.2051 ± 0.0001	0.1327 ± 0.0000	0.0889 ± 0.0000	0.0745 ± 0.0001
TI↑	0.4893 ± 0.0231	0.5023 ± 0.0221	0.4821 ± 0.0186	0.4247 ± 0.0002	0.4450 ± 0.0000	0.5102 ± 0.0000	0.5253 ± 0.0002
DGI↑	0.0243 ± 0.0068	0.0247 ± 0.0068	0.0247 ± 0.0036	0.0098 ± 0.0000	0.0096 ± 0.0000	0.0610 ± 0.0000	0.0327 ± 0.0000
RLI↑	0.2586 ± 0.0086	0.2711 ± 0.021	0.2565 ± 0.0025	0.3121 ± 0.0000	0.2491 ± 0.0000	0.2541 ± 0.0000	0.2622 ± 0.0000
CHI↑	2.0879 ± 0.0443	2.0315 ± 0.0937	2.0973 ± 0.0062	0.5680 ± 0.0003	1.3952 ± 0.0000	1.8244 ± 0.0000	2.1114 ± 0.0000
RTI↓	0.6878 ± 0.1753	0.5812 ± 0.1759	0.7428 ± 0.1425	0.7824 ± 0.0029	1.4506 ± 0.0000	0.5442 ± 0.0000	0.4168 ± 0.0003
WGI↑	0.4604 ± 0.0249	0.4785 ± 0.0275	0.4523 ± 0.0197	0.4316 ± 0.0002	0.4250 ± 0.0000	0.4269 ± 0.0000	0.4976 ± 0.0001
DI↑	0.0025 ± 0.0008	0.0034 ± 0.0012	0.0025 ± 0.0004	0.0025 ± 0.0000	0.0010 ± 0.0000	0.0067 ± 0.0000	0.0034 ± 0.0000
BHI↑	0.0617 ± 0.0125	0.0794 ± 0.0275	0.0582 ± 0.0041	0.2173 ± 0.0000	0.0554 ± 0.0000	0.0586 ± 0.0000	0.0678 ± 0.0000
PBMI↑	0.1118 ± 0.0137	0.1583 ± 0.0829	0.1090 ± 0.0100	0.0926 ± 0.0000	0.1108 ± 0.0000	0.1062 ± 0.0000	0.1324 ± 0.0000
XBI↓	0.3369 ± 0.1914	0.2285 ± 0.1610	0.2881 ± 0.0746	0.6293 ± 0.0001	1.7756 ± 0.0000	0.0478 ± 0.0000	0.1190 ± 0.0000
DBI↓	1.0248 ± 0.0060	0.9943 ± 0.0669	1.0267 ± 0.0021	1.5361 ± 0.0021	1.0918 ± 0.0000	1.0082 ± 0.0000	1.0207 ± 0.0000
LSSRI↑	0.7359 ± 0.0221	0.7077 ± 0.0468	0.7406 ± 0.0029	-0.5657 ± 0.0006	0.3331 ± 0.0000	0.6013 ± 0.0000	0.7474 ± 0.0000
TWI↓	4.3434 ± 0.0656	4.4274 ± 0.1393	4.3293 ± 0.0086	8.5517 ± 0.0019	5.5982 ± 0.0000	4.7475 ± 0.0000	4.3096 ± 0.0000
ACC↑	0.4416 ± 0.0588	0.4822 ± 0.0625	0.4222 ± 0.0463	0.7193 ± 0.0001	0.4793 ± 0.0000	0.5387 ± 0.0000	0.5291 ± 0.0004
NMI↑	0.1529 ± 0.0039	0.1545 ± 0.0050	0.1514 ± 0.0007	0.1003 ± 0.0000	0.1737 ± 0.0000	0.1578 ± 0.0000	0.1505 ± 0.0001
ARI↑	0.0952 ± 0.0096	0.1029 ± 0.0110	0.0914 ± 0.0067	0.0528 ± 0.0001	0.0866 ± 0.0000	0.1226 ± 0.0000	0.1077 ± 0.0002
PageBlocks	FCM	MEC	FSC	2PFCM	BFC	KFCM	CAFCM
WGSS↓	21.8530 ± 0.0000	34.2909 ± 2.9662	41.3223 ± 1.1842	21.8530 ± 0.0000	52.5699 ± 4.7438	31.4679 ± 2.8910	21.5478 ± 0.0000
MRI↓	0.4232 ± 0.0000	0.6254 ± 0.0476	0.5970 ± 0.0128	0.4232 ± 0.0000	0.9579 ± 0.0301	0.6010 ± 0.0541	0.3973 ± 0.0000
GPI↓	0.0532 ± 0.0000	0.1318 ± 0.0150	0.1031 ± 0.0095	0.0532 ± 0.0000	0.1557 ± 0.0040	0.1161 ± 0.0184	0.0475 ± 0.0000
BHGI↑	0.7142 ± 0.0000	0.4501 ± 0.0669	0.5007 ± 0.0268	0.7142 ± 0.0000	0.0441 ± 0.0308	0.4788 ± 0.0757	0.7871 ± 0.0000
CI↓	0.0976 ± 0.0000	0.2499 ± 0.0330	0.2945 ± 0.0085	0.0976 ± 0.0000	0.3822 ± 0.0124	0.2203 ± 0.0370	0.0744 ± 0.0000
TI↑	0.4356 ± 0.0000	0.3122 ± 0.0487	0.3210 ± 0.0123	0.4356 ± 0.0000	0.0253 ± 0.0179	0.3196 ± 0.0523	0.5257 ± 0.0000
DGI↑	0.0342 ± 0.0000	0.0219 ± 0.0061	0.0010 ± 0.0001	0.0342 ± 0.0000	0.0000 ± 0.0000	0.0220 ± 0.0060	0.0327 ± 0.0000
RLI↑	0.2544 ± 0.0000	0.1994 ± 0.0177	0.1406 ± 0.0090	0.2544 ± 0.0000	0.0645 ± 0.0235	0.2085 ± 0.0155	0.2622 ± 0.0000
CHI↑	2.0556 ± 0.0000	0.7092 ± 0.1532	0.1743 ± 0.0122	2.0556 ± 0.0000	0.0407 ± 0.0311	0.8305 ± 0.1698	2.1114 ± 0.0000
RTI↓	1.1244 ± 0.0000	4.4488 ± 7.6595	4.6271 ± 1.2316	1.1244 ± 0.0000	1549.5546 ± 1722.8200	2.3455 ± 1.8063	0.4160 ± 0.0000
WGI↑	0.4171 ± 0.0000	0.1496 ± 0.1103	0.1145 ± 0.1211	0.4171 ± 0.0000	0.0031 ± 0.0075	0.1767 ± 0.0886	0.4978 ± 0.0000
DI↑	0.0034 ± 0.0000	0.0023 ± 0.0006	0.0002 ± 0.0000	0.0034 ± 0.0000	0.0000 ± 0.0000	0.0023 ± 0.0007	0.0034 ± 0.0000
BHI↑	0.0552 ± 0.0000	0.0681 ± 0.0190	0.1957 ± 0.0211	0.0552 ± 0.0000	0.1204 ± 0.0021	0.0655 ± 0.0134	0.0678 ± 0.0000
PBMI↑	0.1047 ± 0.0000	0.0202 ± 0.0061	0.0223 ± 0.0080	0.1047 ± 0.0000	0.0024 ± 0.0041	0.0249 ± 0.0082	0.1323 ± 0.0000
XBI↓	0.1466 ± 0.0000	1.3735 ± 5.1380	139.8571 ± 9.2299	0.1466 ± 0.0000	∞ ± NaN	0.6332 ± 0.4108	0.1190 ± 0.0000
DBI↓	1.1062 ± 0.0000	1.6489 ± 0.5322	3.5630 ± 0.4570	1.1062 ± 0.0000	33.3310 ± 13.4587	1.4613 ± 0.2929	1.0206 ± 0.0000
LSSRI↑	0.7206 ± 0.0000	-0.4349 ± 0.2160	-1.7495 ± 0.0680	0.7206 ±			

TABLE IV

THE MEAN VALUES AND STANDARD DEVIATIONS OF INTERNAL AND EXTERNAL CLUSTER VALIDITY INDICES RESULTING FROM CAFCM, AND THIRTEEN BASELINES ON TEXTURE AND OPTDIGITS, WHERE $N = 3$ AND $M = 15$ IN CAPKM++2.0 AND CAFCM ON TEXTURE, AND $N = 2$ AND $M = 5$ IN CAPKM++2.0 AND CAFCM ON OPTDIGITS.

Texture	KM	KM++	PKM	EWPKM	SC	HC	CAPKM++2.0
WGSS↓	16.3911 ± 1.0559	15.9094 ± 0.6088	15.6292 ± 0.0044	15.6776 ± 0.0029	19.2342 ± 0.4501	16.1971 ± 0.0000	15.5736 ± 0.0004
MRI↓	0.3433 ± 0.0135	0.3375 ± 0.0085	0.3337 ± 0.0003	0.3345 ± 0.0001	0.4125 ± 0.0172	0.3535 ± 0.0000	0.3332 ± 0.0003
GPI↓	0.0097 ± 0.0022	0.0087 ± 0.0014	0.0081 ± 0.0000	0.0082 ± 0.0000	0.0246 ± 0.0054	0.0115 ± 0.0000	0.0079 ± 0.0000
BHGI↑	0.8995 ± 0.0186	0.9092 ± 0.0128	0.9139 ± 0.0002	0.9136 ± 0.0001	0.7962 ± 0.0262	0.8921 ± 0.0000	0.9199 ± 0.0002
CI↓	0.0373 ± 0.0064	0.0338 ± 0.0045	0.0323 ± 0.0001	0.0326 ± 0.0000	0.0709 ± 0.0098	0.0389 ± 0.0000	0.0300 ± 0.0001
TI↑	0.3940 ± 0.0138	0.3986 ± 0.0126	0.3970 ± 0.0008	0.3977 ± 0.0002	0.3895 ± 0.0052	0.4127 ± 0.0000	0.4095 ± 0.0005
DGI↑	0.1157 ± 0.0175	0.1173 ± 0.0210	0.0996 ± 0.0194	0.1064 ± 0.0001	0.1294 ± 0.0043	0.2607 ± 0.0000	0.1067 ± 0.0288
RLI↑	0.2777 ± 0.0023	0.2787 ± 0.0013	0.2793 ± 0.0000	0.2795 ± 0.0000	0.2702 ± 0.0025	0.2764 ± 0.0000	0.2793 ± 0.0000
CHI↑	7.0583 ± 0.4753	7.2822 ± 0.2871	7.4197 ± 0.0024	7.3306 ± 0.0022	5.0688 ± 0.3170	6.5713 ± 0.0000	7.4498 ± 0.0002
RTL↓	1.0800 ± 0.5900	0.8433 ± 0.2548	0.7606 ± 0.0477	0.6440 ± 0.0070	2.2327 ± 0.2134	0.8343 ± 0.0000	0.6207 ± 0.0091
WGI↑	0.4006 ± 0.0169	0.4075 ± 0.0119	0.4072 ± 0.0009	0.4007 ± 0.0003	0.3109 ± 0.0107	0.3707 ± 0.0000	0.4125 ± 0.0005
DI↑	0.0178 ± 0.0036	0.0201 ± 0.0043	0.0190 ± 0.0032	0.0199 ± 0.0000	0.0164 ± 0.0011	0.0464 ± 0.0000	0.0187 ± 0.0050
BHI↑	0.1312 ± 0.0082	0.1371 ± 0.0073	0.1421 ± 0.0024	0.1405 ± 0.0001	0.1340 ± 0.0034	0.1500 ± 0.0000	0.1391 ± 0.0003
PBMI↑	0.5566 ± 0.0672	0.6295 ± 0.0808	0.7082 ± 0.0197	0.6900 ± 0.0008	0.3830 ± 0.0112	0.7264 ± 0.0000	0.6281 ± 0.0032
XBI↓	0.0105 ± 0.0034	0.0097 ± 0.0036	0.0118 ± 0.0036	0.0094 ± 0.0000	0.0119 ± 0.0012	0.0022 ± 0.0000	0.0123 ± 0.0045
DBI↓	1.2223 ± 0.0549	1.1994 ± 0.0333	1.1962 ± 0.0109	1.1921 ± 0.0021	1.4880 ± 0.0449	1.2158 ± 0.0000	1.1751 ± 0.0016
LSSRI↑	1.9518 ± 0.0709	1.9846 ± 0.0417	2.0041 ± 0.0003	1.9921 ± 0.0003	1.6207 ± 0.0742	1.8827 ± 0.0000	2.0082 ± 0.0000
TWI↓	1.4901 ± 0.0960	1.4463 ± 0.0553	1.4208 ± 0.0004	1.4360 ± 0.0004	1.9782 ± 0.1374	1.5801 ± 0.0000	1.4158 ± 0.0000
ACC↑	0.5837 ± 0.0605	0.5955 ± 0.0470	0.6072 ± 0.0145	0.5610 ± 0.0005	0.6464 ± 0.0093	0.6258 ± 0.0000	0.5706 ± 0.0010
NMI↑	0.6298 ± 0.0216	0.6342 ± 0.0157	0.6294 ± 0.0006	0.6057 ± 0.0011	0.7588 ± 0.0102	0.6666 ± 0.0000	0.6313 ± 0.0006
ARI↑	0.4653 ± 0.0467	0.4754 ± 0.0357	0.4777 ± 0.0049	0.4459 ± 0.0011	0.5215 ± 0.0200	0.4884 ± 0.0000	0.4593 ± 0.0016
Texture	FCM	MEC	FSC	2PFCM	BFC	KFCM	CAFCM
WGSS↓	16.0626 ± 0.1793	51.2179 ± 2.9583	33.7848 ± 3.5161	16.0031 ± 0.0000	×	43.7941 ± 1.8668	15.5734 ± 0.0000
MRI↓	0.3346 ± 0.0016	0.5275 ± 0.0003	0.8380 ± 0.0074	0.3341 ± 0.0000	×	0.5434 ± 0.0032	0.3330 ± 0.0000
GPI↓	0.0084 ± 0.0002	0.0781 ± 0.0002	0.0940 ± 0.0048	0.0083 ± 0.0000	×	0.0892 ± 0.0019	0.0079 ± 0.0000
BHGI↑	0.9011 ± 0.0025	0.6874 ± 0.0009	0.1706 ± 0.0110	0.9019 ± 0.0000	×	0.6376 ± 0.0096	0.9199 ± 0.0000
CI↓	0.0369 ± 0.0008	0.1366 ± 0.0002	0.3168 ± 0.0044	0.0367 ± 0.0000	×	0.1483 ± 0.0026	0.0300 ± 0.0000
TI↑	0.3712 ± 0.0004	0.4860 ± 0.0006	0.0812 ± 0.0058	0.3714 ± 0.0000	×	0.4474 ± 0.0097	0.4093 ± 0.0000
DGI↑	0.1211 ± 0.0157	0.0950 ± 0.0019	0.0595 ± 0.0087	0.1263 ± 0.0000	×	0.0953 ± 0.0077	0.0890 ± 0.0000
RLI↑	0.2775 ± 0.0007	0.3644 ± 0.0394	0.1894 ± 0.0040	0.2778 ± 0.0000	×	0.2238 ± 0.0036	0.2793 ± 0.0000
CHI↑	7.1204 ± 0.1057	4.4463 ± 1.2798	0.4649 ± 0.0430	7.1556 ± 0.0000	×	1.4389 ± 0.0820	7.4499 ± 0.0000
RTL↓	1.0617 ± 0.0051	4.5746 ± 6.3519	42.4433 ± 16.7327	1.0594 ± 0.0000	×	60.9281 ± 28.9960	0.6144 ± 0.0000
WGI↑	0.3839 ± 0.0044	0.1331 ± 0.0639	0.0197 ± 0.0169	0.3853 ± 0.0000	×	0.0562 ± 0.0186	0.4123 ± 0.0000
DI↑	0.0165 ± 0.0018	0.0108 ± 0.0000	0.0104 ± 0.0016	0.0170 ± 0.0000	×	0.0109 ± 0.0009	0.0156 ± 0.0000
BHI↑	0.1299 ± 0.0011	0.2549 ± 0.0609	0.5555 ± 0.0426	0.1295 ± 0.0000	×	0.1620 ± 0.0066	0.1391 ± 0.0000
PBMI↑	0.4994 ± 0.0208	0.3232 ± 0.1332	0.1040 ± 0.0082	0.4924 ± 0.0000	×	0.0476 ± 0.0038	0.6284 ± 0.0000
XBI↓	0.0101 ± 0.0045	0.0457 ± 0.0000	0.1044 ± 0.0469	0.0086 ± 0.0000	×	0.0433 ± 0.0065	0.0151 ± 0.0000
DBI↓	1.3566 ± 0.0035	1.2662 ± 0.4884	6.2638 ± 0.9078	1.3552 ± 0.0000	×	4.6500 ± 0.7287	1.1756 ± 0.0000
LSSRI↑	1.9628 ± 0.0151	0.1953 ± 0.0020	-0.7804 ± 0.0872	1.9679 ± 0.0000	×	0.3540 ± 0.0498	2.0082 ± 0.0000
TWI↓	1.4735 ± 0.0199	5.3993 ± 0.0058	8.2005 ± 0.2295	1.4668 ± 0.0000	×	4.9345 ± 0.1425	1.4158 ± 0.0000
ACC↑	0.6330 ± 0.0114	0.1824 ± 0.0003	0.1860 ± 0.0206	0.6367 ± 0.0000	×	0.2036 ± 0.0170	0.5709 ± 0.0000
NMI↑	0.6254 ± 0.0046	0.3779 ± 0.0006	0.1238 ± 0.0232	0.6269 ± 0.0000	×	0.3642 ± 0.0142	0.6313 ± 0.0000
ARI↑	0.5018 ± 0.0102	0.1315 ± 0.0002	0.0376 ± 0.0073	0.5050 ± 0.0000	×	0.1465 ± 0.0120	0.4596 ± 0.0000
Optdigits	KM	KM++	PKM	EWPKM	SC	HC	CAPKM++2.0
WGSS↓	238.0204 ± 3.7684	238.6506 ± 4.5788	235.2651 ± 0.7834	344.0539 ± 5.0062	241.4227 ± 0.0360	237.9126 ± 0.0000	234.8252 ± 0.0000
MRI↓	0.7191 ± 0.0094	0.7199 ± 0.0093	0.7111 ± 0.0025	0.9429 ± 0.0013	0.7281 ± 0.0015	0.7253 ± 0.0000	0.7111 ± 0.0000
GPI↓	0.0189 ± 0.0025	0.0190 ± 0.0026	0.0169 ± 0.0006	0.1919 ± 0.0047	0.0231 ± 0.0005	0.0218 ± 0.0000	0.0168 ± 0.0000
BHGI↑	0.8118 ± 0.0201	0.8130 ± 0.0249	0.8237 ± 0.0063	0.2000 ± 0.0057	0.7793 ± 0.0034	0.7862 ± 0.0000	0.8307 ± 0.0000
CI↓	0.1176 ± 0.0111	0.1162 ± 0.0138	0.1115 ± 0.0045	0.3780 ± 0.0044	0.1251 ± 0.0014	0.1245 ± 0.0000	0.1059 ± 0.0000
TI↑	0.3632 ± 0.0138	0.3669 ± 0.0151	0.3606 ± 0.0087	0.1385 ± 0.0032	0.3568 ± 0.0004	0.3552 ± 0.0000	0.3701 ± 0.0000
DGI↑	0.4874 ± 0.0387	0.4926 ± 0.0475	0.4799 ± 0.0476	0.3499 ± 0.0462	0.6619 ± 0.0100	0.6114 ± 0.0000	0.4134 ± 0.0000
RLI↑	0.1809 ± 0.0017	0.1809 ± 0.0023	0.1820 ± 0.0004	0.1278 ± 0.0011	0.1785 ± 0.0001	0.1791 ± 0.0000	0.1821 ± 0.0000
CHI↑	0.8088 ± 0.0279	0.8042 ± 0.0336	0.8296 ± 0.0060	0.0885 ± 0.0022	0.7446 ± 0.0021	0.7653 ± 0.0000	0.8330 ± 0.0000
RTL↓	1.6654 ± 0.6256	1.4157 ± 0.4323	1.5200 ± 0.2926	17.4298 ± 2.3087	1.0344 ± 0.0013	1.0956 ± 0.0000	1.1413 ± 0.0004
WGI↑	0.2767 ± 0.0121	0.2766 ± 0.0151	0.2826 ± 0.0055	0.0089 ± 0.0020	0.2740 ± 0.0003	0.2671 ± 0.0000	0.2904 ± 0.0000
DI↑	0.1368 ± 0.0121	0.1405 ± 0.0149	0.1331 ± 0.0139	0.1053 ± 0.0137	0.1733 ± 0.0024	0.1692 ± 0.0000	0.1139 ± 0.0000
BHI↑	2.5823 ± 0.0427	2.5976 ± 0.0449	2.5910 ± 0.0087	3.5609 ± 0.0368	2.6041 ± 0.0035	2.6413 ± 0.0000	2.5848 ± 0.0001
PBMI↑	0.1568 ± 0.0067	0.1561 ± 0.0073	0.1547 ± 0.0033	0.1059 ± 0.0047	0.1900 ± 0.0005	0.1596 ± 0.0000	0.1545 ± 0.0001
XBI↓	0.0014 ± 0.0002	0.0013 ± 0.0003	0.0014 ± 0.0003	0.0030 ± 0.0007	0.0007 ± 0.0000	0.0008 ± 0.0000	0.0019 ± 0.0000
DBI↓	1.9179 ± 0.0796	1.8986 ± 0.0961	1.9102 ± 0.0474	4.9440 ± 0.2232	1.8383 ± 0.0047	1.9093 ± 0.0000	1.8543 ± 0.0002
LSSRI↑	-0.2128 ± 0.0356	-0.2187 ± 0.0433	-0.1869 ± 0.0073	-2.4247 ± 0.0255	-0.2950 ± 0.0029	-0.2675 ± 0.0000	-0.1827 ± 0.0000
TWI↓	23.8020 ± 0.3768	23.8651 ± 0.4579	23.5267 ± 0.0783	39.5425 ± 0.0817	24.6730 ± 0.0300	24.3835 ± 0.0000	23.4825 ± 0.0000
ACC↑	0.7537 ± 0.0641	0.7357 ± 0.0528	0.7950 ± 0.0256	0.1741 ± 0.0039	0.8265 ± 0.0003	0.8089 ± 0.0000	0.7914 ± 0.0001
NMI↑	0.7342 ± 0.0272	0.7240 ± 0.0255	0.7486 ± 0.0111	0.1355 ± 0.0007	0.8708 ± 0.0006	0.8250 ± 0.0000	0.7563 ± 0.0002
ARI↑	0.6355 ± 0.0602	0.6160 ± 0.0507	0.6722 ± 0.0250	0.0150 ± 0.0013	0.7799 ± 0.0003	0.7170 ± 0.0000	0.6704 ± 0.0002
Optdigits	FCM	MEC	FSC	2PFCM	BFC	KFCM	CAFCM
WGSS↓	301.2430 ± 10.6738	289.1568 ± 9.2649	387.2978 ± 11.7520	306.0312 ± 0.0000	365.3603 ± 7.7366	287.3822 ± 9.4675	234.8252 ± 0.0000
MRI↓	0.8541 ± 0.0154	0.8345 ± 0.0171	0.9156 ± 0.0119	0.8408 ± 0.0000	0.9824 ± 0.0049	0.8318 ± 0.0184	0.7111 ± 0.0000
GPI↓	0.0935 ± 0.0161	0.0734 ± 0.0161	0.0576 ± 0.0337	0.0846 ± 0.0000	0.0886 ± 0.0019	0.0683 ± 0.0124	0.0168 ± 0.0000
BHGI↑	0.4784 ± 0.0480	0.5364 ± 0.0474	0.3218 ± 0.0492	0.5264 ± 0.0000	0.0517 ± 0.0137	0.5403 ± 0.0571	0.8307 ± 0.0000
CI↓	0.2699 ± 0.0217	0.2515 ± 0.0188	0.3031 ± 0.0220	0.2439 ± 0.0000	0.5344 ± 0.0076	0.2534 ± 0.0279	0.1059 ± 0.0000
TI↑	0.2844 ± 0.0238	0.2984 ± 0.0179	0.1252 ± 0.0392	0.3146 ± 0.0000	0.0224 ± 0.0060	0.2929 ± 0.0274	0.3701 ± 0.0000
DGI↑	0.3498 ± 0.0508	0.3593 ± 0.0487	0.4267 ± 0.0481	0.3305 ± 0.0000	0.2348 ± 0.0281	0.3552 ± 0.0543	0.4135 ± 0.0000
RLI↑	0.1429 ± 0.0101	0.1443 ± 0.0085	0.1151 ± 0.0095	0.1491 ± 0.0000	0.0451 ± 0.0063	0.1427 ± 0.0077	0.1821 ± 0.0000
CHI↑	0.4032 ± 0.0668	0.4028 ± 0.0588	0.0376 ± 0.0156	0.4423 ± 0.0000	0.0280 ± 0.0081	0.4001 ± 0.0538	0.8330 ± 0.0000
RTL↓	5.1299 ± 2.4365	3.3267 ± 1.2337	3.1296 ± 1.1438	4.9275 ± 0.0000	87.9181 ± 47.4428	3.5445 ± 1.4785	1.1414 ± 0.0000
WGI↑	0.0760 ± 0.0263	0.0830 ± 0.0237	0.0459 ± 0.0267	0.0898 ± 0.0000	0.0000 ± 0.0000	0.0866 ± 0.0251	0.2904 ± 0.0000
DI↑	0.1034 ± 0.0149	0.1065 ± 0.0149	0.1325 ± 0.0150	0.0960 ± 0.0000	0.0732 ± 0.0087	0.1060 ± 0.0155	0.1139 ± 0.0000
BHI↑	3.0998 ± 0.2102	3.0147 ± 0.2178	2.8654 ± 0.5831	3.3187 ± 0.0000	4.6291 ± 0.0381	3.0222 ± 0.2087	2.5848 ± 0.0000
PBMI↑	0.1806 ± 0.0537	0.1209 ± 0.0293	0.2901 ± 0.0719	0.1531 ± 0.0000	0.0066 ± 0.0021	0.1082 ± 0.0231	0.1544 ± 0.0000
XBI↓	0.0029 ± 0.0010	0.0027 ± 0.0010	0.0019 ± 0.0003	0.0030 ± 0.0000	0.0066 ± 0.0013	0.0028 ± 0.0012	0.0019 ± 0.0000
DBI↓	2.9943 ± 0.3742	2.6679 ± 0.2418	2.3283 ± 0.3616	3.3505 ± 0.0000	13.8393 ± 2.0233	2.7372 ± 0.2927	1.8541 ± 0.0000
LSSRI↑	-1.1949 ± 0.1293	-1.0071 ± 0.1217	-3.8470 ± 0.5176	-1.2218 ± 0.0000	-3.6155 ± 0.2831	-0.9709 ± 0.1269	-0.1827 ± 0.0000
TWI↓	33.0074 ± 0.9936	31.4988 ± 1.0204	42.0430 ± 0.4150	33.2459 ± 0.0000	41.8754 ± 0.3268	31.1890 ± 1.0839	23.4825 ± 0.0000

TABLE V

THE MEAN VALUES AND STANDARD DEVIATIONS OF INTERNAL AND EXTERNAL CLUSTER VALIDITY INDICES RESULTING FROM CAFCM, AND THIRTEEN BASELINES ON EGS AND LR, WHERE $N = 2$ AND $M = 5$ IN CAPKM++2.0 AND CAFCM ON EGS, AND $N = 3$ AND $M = 15$ IN CAPKM++2.0 AND CAFCM ON LR.

EGS	KM	KM++	PKM	EWPKM	SC	HC	CAPKM++2.0
WGSS↓	699.6124 ± 0.3592	699.5962 ± 0.3487	699.4982 ± 0.4711	699.6561 ± 0.0000	700.3543 ± 0.0001	708.1015 ± 0.0000	699.3998 ± 0.0000
MRI↓	0.9233 ± 0.0002	0.9233 ± 0.0002	0.9233 ± 0.0006	0.9236 ± 0.0000	0.9270 ± 0.0000	0.9643 ± 0.0000	0.9231 ± 0.0000
GPI↓	0.1883 ± 0.0001	0.1883 ± 0.0001	0.1883 ± 0.0005	0.1887 ± 0.0000	0.1914 ± 0.0000	0.2215 ± 0.0000	0.1882 ± 0.0000
BHGI↑	0.2466 ± 0.0005	0.2467 ± 0.0004	0.2467 ± 0.0018	0.2452 ± 0.0000	0.2345 ± 0.0000	0.1109 ± 0.0000	0.2471 ± 0.0000
CI↓	0.3640 ± 0.0004	0.3639 ± 0.0004	0.3639 ± 0.0010	0.3645 ± 0.0000	0.3708 ± 0.0000	0.4375 ± 0.0000	0.3637 ± 0.0000
TI↑	0.1744 ± 0.0003	0.1744 ± 0.0003	0.1745 ± 0.0013	0.1734 ± 0.0000	0.1658 ± 0.0000	0.0783 ± 0.0000	0.1747 ± 0.0000
DGI↑	0.3843 ± 0.0069	0.3933 ± 0.0570	0.3486 ± 0.0166	0.4417 ± 0.0000	0.2612 ± 0.0000	0.5407 ± 0.0000	0.3449 ± 0.0000
RLI↑	0.2231 ± 0.0034	0.2233 ± 0.0033	0.2242 ± 0.0017	0.2257 ± 0.0000	0.2131 ± 0.0000	0.1528 ± 0.0000	0.2246 ± 0.0000
CHI↑	0.0834 ± 0.0006	0.0835 ± 0.0005	0.0836 ± 0.0007	0.0833 ± 0.0000	0.0783 ± 0.0000	0.0401 ± 0.0000	0.0838 ± 0.0000
RTI↓	2.9960 ± 0.0201	2.9950 ± 0.0195	2.9899 ± 0.0276	3.0018 ± 0.0000	3.1912 ± 0.0000	5.8545 ± 0.0000	2.9841 ± 0.0000
WGI↑	0.1328 ± 0.0003	0.1328 ± 0.0002	0.1328 ± 0.0008	0.1322 ± 0.0000	0.1265 ± 0.0000	0.0720 ± 0.0000	0.1330 ± 0.0000
DI↑	0.1005 ± 0.0139	0.1029 ± 0.0121	0.0930 ± 0.0043	0.1184 ± 0.0000	0.0677 ± 0.0000	0.1427 ± 0.0000	0.0921 ± 0.0000
BHI↑	0.9095 ± 0.0005	0.9095 ± 0.0005	0.9093 ± 0.0006	0.9096 ± 0.0000	0.9139 ± 0.0000	0.9408 ± 0.0000	0.9092 ± 0.0000
PBMI↑	0.0824 ± 0.0005	0.0824 ± 0.0005	0.0825 ± 0.0007	0.0822 ± 0.0000	0.0774 ± 0.0000	0.0422 ± 0.0000	0.0827 ± 0.0000
XBI↓	0.0015 ± 0.0005	0.0014 ± 0.0004	0.0017 ± 0.0001	0.0011 ± 0.0000	0.0030 ± 0.0000	0.0007 ± 0.0000	0.0017 ± 0.0000
DBI↓	3.4269 ± 0.0109	3.4264 ± 0.0106	3.4236 ± 0.0154	3.4309 ± 0.0000	3.5355 ± 0.0000	4.7719 ± 0.0000	3.4204 ± 0.0000
LSSRI↑	-2.4836 ± 0.0067	-2.4833 ± 0.0065	-2.4815 ± 0.009	-2.4855 ± 0.0000	-2.5467 ± 0.0000	-3.2157 ± 0.0000	-2.4796 ± 0.0000
TWI↓	349.8062 ± 0.1796	349.7981 ± 0.1744	349.7503 ± 0.2395	349.8587 ± 0.0000	351.4634 ± 0.0002	364.3754 ± 0.0000	349.6999 ± 0.0000
ACC↑	0.6190 ± 0.1107	0.6145 ± 0.1085	0.5998 ± 0.0290	0.5015 ± 0.0000	0.7968 ± 0.0001	0.6062 ± 0.0000	0.5898 ± 0.0001
NMI↑	0.0941 ± 0.1468	0.0885 ± 0.1443	0.0357 ± 0.0352	0.0000 ± 0.0000	0.3139 ± 0.0001	0.0729 ± 0.0000	0.0262 ± 0.0000
ARI↑	0.1046 ± 0.1599	0.0985 ± 0.1572	0.0430 ± 0.0398	-0.0001 ± 0.0000	0.3523 ± 0.0002	0.0406 ± 0.0000	0.0322 ± 0.0001
EGS	FCM	MEC	FSC	2PFCM	BFC	KFCM	CAFCM
WGSS↓	701.7638 ± 2.3880	707.6171 ± 3.8777	713.7808 ± 19.2256	700.2104 ± 0.0000 ×		706.7937 ± 3.7233	699.3998 ± 0.0000
MRI↓	0.9263 ± 0.0033	0.9344 ± 0.0048	0.9493 ± 0.0346	0.9244 ± 0.0000 ×		0.9334 ± 0.0046	0.9231 ± 0.0000
GPI↓	0.1908 ± 0.0028	0.1976 ± 0.0040	0.2091 ± 0.0278	0.1893 ± 0.0000 ×		0.1968 ± 0.0039	0.1882 ± 0.0000
BHGI↑	0.2367 ± 0.0110	0.2095 ± 0.0162	0.1630 ± 0.1117	0.2427 ± 0.0000 ×		0.2129 ± 0.0155	0.2471 ± 0.0000
CI↓	0.3695 ± 0.0060	0.3842 ± 0.0088	0.4100 ± 0.0613	0.3659 ± 0.0000 ×		0.3824 ± 0.0085	0.3637 ± 0.0000
TI↑	0.1674 ± 0.0078	0.1481 ± 0.0114	0.1152 ± 0.0790	0.1716 ± 0.0000 ×		0.1505 ± 0.0109	0.1747 ± 0.0000
DGI↑	0.3672 ± 0.0345	0.3764 ± 0.0380	0.3746 ± 0.0615	0.3332 ± 0.0000 ×		0.3769 ± 0.0370	0.3449 ± 0.0000
RLI↑	0.2136 ± 0.0106	0.1894 ± 0.0158	0.1595 ± 0.0861	0.2234 ± 0.0000 ×		0.1923 ± 0.0150	0.2246 ± 0.0000
CHI↑	0.0796 ± 0.0041	0.0697 ± 0.0059	0.0522 ± 0.0351	0.0823 ± 0.0000 ×		0.0709 ± 0.0057	0.0838 ± 0.0000
RTI↓	3.1493 ± 0.1793	3.6117 ± 0.3095	66.5073 ± 141.6230	3.0367 ± 0.0000 ×		3.5469 ± 0.2906	2.9841 ± 0.0000
WGI↑	0.1282 ± 0.0051	0.1155 ± 0.0076	0.0853 ± 0.0564	0.1310 ± 0.0000 ×		0.1171 ± 0.0072	0.1330 ± 0.0000
DI↑	0.0960 ± 0.0096	0.0980 ± 0.0104	0.0981 ± 0.0178	0.0865 ± 0.0000 ×		0.0979 ± 0.0101	0.0921 ± 0.0000
BHI↑	0.9127 ± 0.0035	0.9212 ± 0.0051	0.9383 ± 0.0293	0.9104 ± 0.0000 ×		0.9202 ± 0.0049	0.9092 ± 0.0000
PBMI↑	0.0786 ± 0.0040	0.0688 ± 0.0058	0.0523 ± 0.0350	0.0812 ± 0.0000 ×		0.0700 ± 0.0056	0.0827 ± 0.0000
XBI↓	0.0016 ± 0.0004	0.0015 ± 0.0003	0.0016 ± 0.0007	0.0019 ± 0.0000 ×		0.0015 ± 0.0003	0.0017 ± 0.0000
DBI↓	3.5118 ± 0.0971	3.7587 ± 0.1605	10.6748 ± 12.2112	3.4507 ± 0.0000 ×		3.7253 ± 0.1515	3.4204 ± 0.0000
LSSRI↑	-2.5320 ± 0.0539	-2.6669 ± 0.0852	-3.8010 ± 1.8519	-2.4971 ± 0.0000 ×		-2.6492 ± 0.0809	-2.4796 ± 0.0000
TWI↓	351.0553 ± 1.3317	354.3084 ± 1.9544	360.6021 ± 12.3114	350.1689 ± 0.0000 ×		353.9031 ± 1.8724	349.6999 ± 0.0000
ACC↑	0.6705 ± 0.0998	0.6219 ± 0.0712	0.6703 ± 0.2042	0.5639 ± 0.0000 ×		0.6214 ± 0.0813	0.5898 ± 0.0000
NMI↑	0.1361 ± 0.1249	0.0664 ± 0.0659	0.2577 ± 0.361	0.0133 ± 0.0000 ×		0.0715 ± 0.0817	0.0262 ± 0.0000
ARI↑	0.1553 ± 0.1377	0.0792 ± 0.0764	0.2784 ± 0.3861	0.0162 ± 0.0000 ×		0.0848 ± 0.0940	0.0322 ± 0.0000
LR	KM	KM++	PKM	EWPKM	SC	HC	CAPKM++2.0
WGSS↓	172.2610 ± 1.2342	172.2106 ± 1.2526	172.5354 ± 0.8054	285.7491 ± 1.2048	320.8225 ± 3.7651	177.5555 ± 0.0000	169.7897 ± 0.094
MRI↓	0.5847 ± 0.0037	0.5843 ± 0.0033	0.5844 ± 0.0018	0.8217 ± 0.0012	0.8209 ± 0.0086	0.6268 ± 0.0000	0.5804 ± 0.0014
GPI↓	0.0070 ± 0.0003	0.0070 ± 0.0003	0.0068 ± 0.0001	0.0358 ± 0.0006	0.1081 ± 0.0113	0.0131 ± 0.0000	0.0067 ± 0.0002
BHGI↑	0.8367 ± 0.0066	0.8382 ± 0.0055	0.8341 ± 0.0040	0.3671 ± 0.0028	0.4255 ± 0.0235	0.7685 ± 0.0000	0.8458 ± 0.0022
CI↓	0.1072 ± 0.0034	0.1063 ± 0.0029	0.1092 ± 0.0021	0.3042 ± 0.0011	0.2975 ± 0.0098	0.1304 ± 0.0000	0.1025 ± 0.0009
TI↑	0.2446 ± 0.0044	0.2466 ± 0.0049	0.2382 ± 0.0033	0.1235 ± 0.0014	0.2602 ± 0.0107	0.2590 ± 0.0000	0.2497 ± 0.0019
DGI↑	0.2086 ± 0.0051	0.2084 ± 0.0045	0.2093 ± 0.0046	0.1637 ± 0.0007	0.3352 ± 0.0058	0.2015 ± 0.0000	0.2088 ± 0.0011
RLI↑	0.1528 ± 0.0003	0.1529 ± 0.0004	0.1529 ± 0.0002	0.1061 ± 0.0002	0.0817 ± 0.0026	0.1481 ± 0.0000	0.1534 ± 0.0000
CHI↑	1.7576 ± 0.0197	1.7584 ± 0.0201	1.7531 ± 0.0129	0.4214 ± 0.0020	0.2304 ± 0.0177	1.4861 ± 0.0000	1.7976 ± 0.0015
RTI↓	1.2844 ± 0.1338	1.2616 ± 0.1410	1.4320 ± 0.1503	18.7362 ± 2.7223	4.2300 ± 0.3628	1.9338 ± 0.0000	1.1236 ± 0.0278
WGI↑	0.2420 ± 0.0046	0.2434 ± 0.0054	0.2391 ± 0.0029	0.0021 ± 0.0004	0.0891 ± 0.0077	0.1982 ± 0.0000	0.2494 ± 0.0024
DI↑	0.0455 ± 0.0010	0.0456 ± 0.0010	0.0456 ± 0.0007	0.0408 ± 0.0000	0.0623 ± 0.0011	0.0405 ± 0.0000	0.0446 ± 0.0011
BHI↑	0.1399 ± 0.0023	0.1395 ± 0.0022	0.1409 ± 0.0012	0.2665 ± 0.0020	0.0572 ± 0.0040	0.1380 ± 0.0000	0.1382 ± 0.0014
PBMI↑	0.0061 ± 0.0004	0.0061 ± 0.0004	0.0061 ± 0.0002	0.0042 ± 0.0002	0.0040 ± 0.0001	0.0059 ± 0.0000	0.0059 ± 0.0000
XBI↓	0.0016 ± 0.0000	0.0015 ± 0.0000	0.0016 ± 0.0000	0.0030 ± 0.0000	0.0009 ± 0.0000	0.0017 ± 0.0000	0.0015 ± 0.0000
DBI↓	1.6843 ± 0.0403	1.6787 ± 0.0419	1.7244 ± 0.0275	6.1901 ± 0.1554	1.0860 ± 0.0279	1.7262 ± 0.0000	1.6366 ± 0.0269
LSSRI↑	0.5639 ± 0.0112	0.5643 ± 0.0114	0.5614 ± 0.0073	-0.8641 ± 0.0048	-1.4710 ± 0.0775	0.3961 ± 0.0000	0.5864 ± 0.0009
TWI↓	6.6254 ± 0.0475	6.6235 ± 0.0482	6.6361 ± 0.0310	12.8526 ± 0.0184	14.8516 ± 0.2144	7.3487 ± 0.0000	6.5304 ± 0.0036
ACC↑	0.2561 ± 0.0097	0.2582 ± 0.0087	0.2621 ± 0.0061	0.0943 ± 0.0011	0.1279 ± 0.0114	0.2600 ± 0.0000	0.2574 ± 0.0048
NMI↑	0.3562 ± 0.0051	0.3538 ± 0.0058	0.3528 ± 0.0037	0.0685 ± 0.0012	0.2703 ± 0.0235	0.4082 ± 0.0000	0.3608 ± 0.0011
ARI↑	0.1319 ± 0.0057	0.1317 ± 0.0055	0.1367 ± 0.0035	0.0152 ± 0.0003	0.0075 ± 0.0026	0.1293 ± 0.0000	0.1294 ± 0.0024
LR	FCM	MEC	FSC	2PFCM	BFC	KFCM	CAFCM
WGSS↓	303.7112 ± 20.1367	257.0694 ± 8.1591	313.2757 ± 13.1218	314.2095 ± 0.0000	300.3002 ± 15.1015	240.5271 ± 7.1036	169.6638 ± 0.0000
MRI↓	0.8241 ± 0.0063	0.8017 ± 0.0136	0.9774 ± 0.0202	0.8390 ± 0.0000	0.9356 ± 0.0113	0.7822 ± 0.0172	0.5805 ± 0.0000
GPI↓	0.1415 ± 0.0062	0.1117 ± 0.0165	0.1657 ± 0.0108	0.1339 ± 0.0000	0.0353 ± 0.0012	0.0782 ± 0.0181	0.0068 ± 0.0000
BHGI↑	0.3968 ± 0.0179	0.4440 ± 0.0293	0.0432 ± 0.0425	0.3554 ± 0.0000	0.1331 ± 0.0229	0.4781 ± 0.0358	0.8456 ± 0.0000
CI↓	0.2807 ± 0.0084	0.2571 ± 0.0129	0.4552 ± 0.0218	0.3007 ± 0.0000	0.4027 ± 0.0092	0.2450 ± 0.0146	0.1022 ± 0.0000
TI↑	0.2722 ± 0.0193	0.2796 ± 0.0117	0.0253 ± 0.0247	0.2291 ± 0.0000	0.0380 ± 0.0066	0.2582 ± 0.0158	0.2508 ± 0.0000
DGI↑	0.1660 ± 0.0128	0.1806 ± 0.0065	0.1476 ± 0.0085	0.1204 ± 0.0000	0.0000 ± 0.0000	0.1861 ± 0.0041	0.2073 ± 0.0000
RLI↑	0.1034 ± 0.0133	0.1234 ± 0.0079	0.0635 ± 0.0044	0.1118 ± 0.0000	0.0589 ± 0.0064	0.1252 ± 0.0060	0.1534 ± 0.0000
CHI↑	0.4078 ± 0.1115	0.6385 ± 0.0091	0.1026 ± 0.0152	0.4931 ± 0.0000	0.1064 ± 0.0256	0.7139 ± 0.0875	1.7997 ± 0.0000
RTI↓	91.3596 ± 73.4346	9.9121 ± 5.4788	27.6427 ± 11.5610	197.5310 ± 0.0000	129.7907 ± 73.5306	5.2486 ± 1.7978	1.0954 ± 0.0000
WGI↑	0.0172 ± 0.0208	0.0068 ± 0.0060	0.0008 ± 0.0006	0.0239 ± 0.0000	0.0000 ± 0.0000	0.0195 ± 0.0092	0.2523 ± 0.0000
DI↑	0.0353 ± 0.0004	0.0368 ± 0.0010	0.0299 ± 0.0000	0.0351 ± 0.0000	0.0000 ± 0.0000	0.0376 ± 0.0012	0.0454 ± 0.0000
BHI↑	0.2199 ± 0.0577	0.1615 ± 0.0115	0.2843 ± 0.0217	0.1752 ± 0.0000	0.3495 ± 0.0092	0.1584 ± 0.0105	0.1381 ± 0.0000
PBMI↑	0.0028 ± 0.0018	0.0035 ± 0.0008	0.0034 ± 0.0011	0.0041 ± 0.0000	0.0005 ± 0.0002	0.0030 ± 0.0010	0.0060 ± 0.0000
XBI↓	0.0033 ± 0.0001	0.0029 ± 0.0001	0.0039 ± 0.0000	0.0032 ± 0.0000	Inf ± NaN	0.0026 ± 0.0001	0.0015 ± 0.0000
DBI↓	8.3490 ± 4.9826	2.7479 ± 0.2600	5.8008 ± 0.4879	8.2692 ± 0.0000	11.0919 ± 2.4470	2.4005 ± 0.1712	1.6390 ± 0.0000
LSSRI↑	-1.2400 ± 0.1030	-0.7709 ± 0.1309	-2.4892 ± 0.1160	-1.0931 ± 0.0000	-2.2693 ± 0.2487	-0.4841 ± 0.1146	0.5876 ± 0.0000
TWI↓	14.1600 ± 0.3321	12.4791 ± 0.5243	16.8622 ± 0.1510	13.6830 ± 0.0000	16.5212 ±		

REFERENCES

- [1] A. K. Jain, M. N. Murty, and P. J. Flynn, "Data clustering: a review," *ACM Computing Surveys*, vol. 31, no. 3, pp. 264–323, 1999.
- [2] A. K. Jain, "Data clustering: 50 years beyond k-means," *Pattern Recognition Letters*, vol. 31, no. 8, pp. 651–666, 2010.
- [3] R. Xu and D. Wunsch, "Survey of clustering algorithms," *IEEE Transactions on Neural Networks*, vol. 16, no. 3, pp. 645–678, 2005.
- [4] X. Peng, J. Feng, J. T. Zhou, Y. Lei, and S. Yan, "Deep subspace clustering," *IEEE Transactions on Neural Networks and Learning Systems*, vol. 31, no. 12, pp. 5509–5521, 2020.
- [5] S. Zeng, X. Duan, H. Li, J. Bai, Y. Tang, and Z. Wang, "A sparse framework for robust possibilistic k-subspace clustering," *IEEE Transactions on Fuzzy Systems*, 2023, in press.
- [6] L. Jing, M. K. Ng, and J. Z. Huang, "An entropy weighting k-means algorithm for subspace clustering of high-dimensional sparse data," *IEEE Transactions on Knowledge and Data Engineering*, vol. 19, no. 8, pp. 1026–1041, 2007.
- [7] S. Chakraborty, D. Paul, S. Das, and J. Xu, "Entropy weighted power k-means clustering," in *International Conference on Artificial Intelligence and Statistics*. PMLR, 2020, pp. 691–701.
- [8] S. Chakraborty and S. Das, "Detecting meaningful clusters from high-dimensional data: A strongly consistent sparse center-based clustering approach," *IEEE Transactions on Pattern Analysis and Machine Intelligence*, 2023, in press.
- [9] J. B. M. Benjamin and M.-S. Yang, "Weighted multiview possibilistic c-means clustering with L2 regularization," *IEEE Transactions on Fuzzy Systems*, vol. 30, no. 5, pp. 1357–1370, 2022.
- [10] J. Yang and C.-T. Lin, "Multi-view adjacency-constrained hierarchical clustering," *IEEE Transactions on Emerging Topics in Computational Intelligence*, vol. 7, no. 4, pp. 1126–1138, 2023.
- [11] P. Macnaughton-Smith, W. Williams, M. Dale, and L. Mockett, "Dissimilarity analysis: a new technique of hierarchical sub-division," *Nature*, vol. 202, no. 4936, pp. 1034–1035, 1964.
- [12] S. C. Johnson, "Hierarchical clustering schemes," *Psychometrika*, vol. 32, no. 3, pp. 241–254, 1967.
- [13] S. Lloyd, "Least squares quantization in PCM," *IEEE Transactions on Information Theory*, vol. 28, no. 2, pp. 129–137, 1982.
- [14] J. Wang, "A linear assignment clustering algorithm based on the least similar cluster representatives," *IEEE Trans. Systems, Man and Cybernetics, Part A: Systems and Humans*, vol. 29, no. 1, pp. 100–104, 1999.
- [15] M. Tiwari, M. J. Zhang, J. Mayclin, S. Thrun, C. Piech, and I. Shomorony, "Banditpam: Almost linear time k-medoids clustering via multi-armed bandits," in *Advances in Neural Information Processing Systems*, vol. 33, 2020, pp. 10211–10222.
- [16] B. Zhang, "Generalized k-harmonic means–dynamic weighting of data in unsupervised learning," in *Proceedings of the 2001 SIAM International Conference on Data Mining*. SIAM, 2001, pp. 1–13.
- [17] J. Shi and J. Malik, "Normalized cuts and image segmentation," *IEEE Transactions on Pattern Analysis and Machine Intelligence*, vol. 22, no. 8, pp. 888–905, 2000.
- [18] A. Ng, M. Jordan, and Y. Weiss, "On spectral clustering: Analysis and an algorithm," in *Advances in Neural Information Processing Systems*, T. Dietterich, S. Becker, and Z. Ghahramani, Eds., vol. 14. MIT Press, 2001.
- [19] Q. Wang, Z. Qin, F. Nie, and X. Li, "Spectral embedded adaptive neighbors clustering," *IEEE Transactions on Neural Networks and Learning Systems*, vol. 30, no. 4, pp. 1265–1271, 2018.
- [20] J. Bilmes, "A gentle tutorial of the EM algorithm and its application to parameter estimation for Gaussian mixture and hidden Markov models," International Computer Science Institute, Tech. Rep. TR-97-021, 1997.
- [21] D. Comaniciu and P. Meer, "Mean shift: A robust approach toward feature space analysis," *IEEE Transactions on Pattern Analysis and Machine Intelligence*, vol. 24, no. 5, pp. 603–619, 2002.
- [22] A. Becchini, F. Marcelloni, and A. Renda, "TSF-DBSCAN: A novel fuzzy density-based approach for clustering unbounded data streams," *IEEE Transactions on Fuzzy Systems*, vol. 30, no. 3, pp. 623–637, 2022.
- [23] A. Cornuéjols, C. Wemmer, P. Gancarski, and Y. Bennani, "Collaborative clustering: Why, when, what and how," *Information Fusion*, vol. 39, pp. 81–95, 2018.
- [24] X. Yang, C. Deng, Z. Dang, and D. Tao, "Deep multiview collaborative clustering," *IEEE Transactions on Neural Networks and Learning Systems*, vol. 34, no. 1, pp. 516–526, 2023.
- [25] J. Xu and K. Lange, "Power k-means clustering," in *International Conference on Machine Learning*. PMLR, 2019, pp. 6921–6931.
- [26] H. Li and J. Wang, "Collaborative annealing power k-means++ clustering," *Knowledge-Based Systems*, vol. 255, p. 109593, 2022.
- [27] —, "CAPKM++ 2.0: An upgraded version of the collaborative annealing power k-means++ clustering algorithm," *Knowledge-Based Systems*, p. 110241, 2023.
- [28] R. Krishnapuram and J. M. Keller, "A possibilistic approach to clustering," *IEEE Transactions on Fuzzy Systems*, vol. 1, no. 2, pp. 98–110, 1993.
- [29] E. H. Ruspini, J. C. Bezdek, and J. M. Keller, "Fuzzy clustering: A historical perspective," *IEEE Computational Intelligence Magazine*, vol. 14, no. 1, pp. 45–55, 2019.
- [30] M.-S. Yang and C.-Y. Lai, "A robust automatic merging possibilistic clustering method," *IEEE Transactions on Fuzzy Systems*, vol. 19, no. 1, pp. 26–41, 2010.
- [31] K. D. Koutroumbas, S. D. Xenaki, and A. A. Rontogiannis, "On the convergence of the sparse possibilistic c-means algorithm," *IEEE Transactions on Fuzzy Systems*, vol. 26, no. 1, pp. 324–337, 2017.
- [32] J. C. Bezdek, *Pattern Recognition with Fuzzy Objective Function Algorithms*. USA: Kluwer Academic Publishers, 1981.
- [33] Y. Lin and S. Chen, "A centroid auto-fused hierarchical fuzzy c-means clustering," *IEEE Transactions on Fuzzy Systems*, vol. 29, no. 7, pp. 2006–2017, 2020.
- [34] Z. Bian, F.-L. Chung, and S. Wang, "Fuzzy density peaks clustering," *IEEE Transactions on Fuzzy Systems*, vol. 29, no. 7, pp. 1725–1738, 2021.
- [35] J. Zhou, W. Pedrycz, C. Gao, Z. Lai, J. Wan, and Z. Ming, "Robust jointly sparse fuzzy clustering with neighborhood structure preservation," *IEEE Transactions on Fuzzy Systems*, vol. 30, no. 4, pp. 1073–1087, 2022.
- [36] S. Song, Z. Jia, J. Yang, and N. Kasabov, "Image segmentation based on fuzzy low-rank structural clustering," *IEEE Transactions on Fuzzy Systems*, 2023, in press.
- [37] Q. Chen, F. Nie, W. Yu, and X. Li, " $\ell_{2,p}$ -norm and mahalanobis distance based robust fuzzy c-means," *IEEE Transactions on Fuzzy Systems*, 2023, in press.
- [38] D. L. Pham and J. L. Prince, "An adaptive fuzzy c-means algorithm for image segmentation in the presence of intensity inhomogeneities," *Pattern Recognition Letters*, vol. 20, no. 1, pp. 57–68, 1999.
- [39] R. J. Hathaway, J. C. Bezdek, and Y. Hu, "Generalized fuzzy c-means clustering strategies using l_p norm distances," *IEEE Transactions on Fuzzy Systems*, vol. 8, no. 5, pp. 576–582, 2000.
- [40] L. Szilágyi, Z. Benyo, S. M. Szilágyi, and H. Adam, "MR brain image segmentation using an enhanced fuzzy c-means algorithm," in *Proceedings of the 25th Annual International Conference of the IEEE Engineering in Medicine and Biology Society*, vol. 1. IEEE, 2003, pp. 724–726.
- [41] W. Cai, S. Chen, and D. Zhang, "Fast and robust fuzzy c-means clustering algorithms incorporating local information for image segmentation," *Pattern Recognition*, vol. 40, no. 3, pp. 825–838, 2007.
- [42] C.-H. Li, W.-C. Huang, B.-C. Kuo, and C.-C. Hung, "A novel fuzzy weighted c-means method for image classification," *International Journal of Fuzzy Systems*, vol. 10, no. 3, pp. 168–173, 2008.
- [43] C.-C. Hung, S. Kulkarni, and B.-C. Kuo, "A new weighted fuzzy c-means clustering algorithm for remotely sensed image classification," *IEEE Journal of Selected Topics in Signal Processing*, vol. 5, no. 3, pp. 543–553, 2010.
- [44] L. Zhu, F.-L. Chung, and S. Wang, "Generalized fuzzy c-means clustering algorithm with improved fuzzy partitions," *IEEE Transactions on Systems, Man, and Cybernetics, Part B (Cybernetics)*, vol. 39, no. 3, pp. 578–591, 2009.
- [45] S. Krinidis and V. Chatzis, "A robust fuzzy local information c-means clustering algorithm," *IEEE Transactions on Image Processing*, vol. 19, no. 5, pp. 1328–1337, 2010.
- [46] T. C. Glenn, A. Zare, and P. D. Gader, "Bayesian fuzzy clustering," *IEEE Transactions on Fuzzy Systems*, vol. 23, no. 5, pp. 1545–1561, 2014.
- [47] J. Fan, J. Wang, and M. Han, "Cooperative coevolution for large-scale optimization based on kernel fuzzy clustering and variable trust region methods," *IEEE Transactions on Fuzzy Systems*, vol. 22, no. 4, pp. 829–839, Aug 2014.
- [48] T. W. Cheng, D. B. Goldgof, and L. O. Hall, "Fast fuzzy clustering," *Fuzzy Sets and Systems*, vol. 93, no. 1, pp. 49–56, 1998.
- [49] H. Hou and S. Liu, "An improved fuzzy c-means algorithm based on genetic algorithm," *Computer Engineering*, vol. 31, no. 17, pp. 152–154, 2005.
- [50] J. Yu, P. Guo, P. Chen, Z. Zhang, and W. Ruan, "Remote sensing image classification based on improved fuzzy c-means," *Geo-spatial Information Science*, vol. 11, no. 2, pp. 90–94, 2008.

- [51] D.-W. Kim, K. H. Lee, and D. Lee, "A novel initialization scheme for the fuzzy c-means algorithm for color clustering," *Pattern Recognition Letters*, vol. 25, no. 2, pp. 227–237, 2004.
- [52] K. S. Tan, W. H. Lim, and N. A. M. Isa, "Novel initialization scheme for fuzzy c-means algorithm on color image segmentation," *Applied Soft Computing*, vol. 13, no. 4, pp. 1832–1852, 2013.
- [53] H. Yang, J. Peng, B. Xia, and D. Zhang, "Remote sensing classification using fuzzy c-means clustering with spatial constraints based on markov random field," *European Journal of Remote Sensing*, vol. 46, no. 1, pp. 305–316, 2013.
- [54] J. Fan and J. Wang, "A two-phase fuzzy clustering algorithm based on neurodynamic optimization with its application for PolSAR image segmentation," *IEEE Transactions on Fuzzy Systems*, vol. 26, no. 1, pp. 72–83, Feb 2018.
- [55] M. N. Ahmed, S. M. Yamany, N. Mohamed, A. A. Farag, and T. Moriarty, "A modified fuzzy c-means algorithm for bias field estimation and segmentation of MRI data," *IEEE Transactions on Medical Imaging*, vol. 21, no. 3, pp. 193–199, 2002.
- [56] S. Chen and D. Zhang, "Robust image segmentation using fcm with spatial constraints based on new kernel-induced distance measure," *IEEE Transactions on Systems, Man, and Cybernetics, Part B (Cybernetics)*, vol. 34, no. 4, pp. 1907–1916, 2004.
- [57] J. C. Dunn, "A fuzzy relative of the isodata process and its use in detecting compact well-separated clusters," *Journal of Cybernetics*, vol. 3, no. 3, pp. 32–57, 1973.
- [58] J. Kennedy and R. Eberhart, "Particle swarm optimization," in *Proceedings of ICNN'95-International Conference on Neural Networks*, vol. 4. IEEE, 1995, pp. 1942–1948.
- [59] H. Che, J. Wang, and A. Cichocki, "Sparse signal reconstruction via collaborative neurodynamic optimization," *Neural Networks*, vol. 154, pp. 255–269, 2022.
- [60] J. Li, K. Cheng, S. Wang, F. Morstatter, R. P. Trevino, J. Tang, and H. Liu, "Feature selection: A data perspective," *ACM Computing Surveys (CSUR)*, vol. 50, no. 6, p. 94, 2018.
- [61] J. Alcalá-Fdez, A. Fernández, J. Luengo, J. Derrac, S. García, L. Sánchez, and F. Herrera, "KEEL data-mining software tool: data set repository, integration of algorithms and experimental analysis framework," *Journal of Multiple-Valued Logic & Soft Computing*, vol. 17, 2011.
- [62] V. Arzamasov, K. Böhm, and P. Jochem, "Towards concise models of grid stability," in *2018 IEEE International Conference on Communications, Control, and Computing Technologies for Smart Grids (SmartGridComm)*. IEEE, 2018, pp. 1–6.
- [63] P. W. Frey and D. J. Slate, "Letter recognition using holland-style adaptive classifiers," *Machine Learning*, vol. 6, pp. 161–182, 1991.
- [64] G. Gan and J. Wu, "A convergence theorem for the fuzzy subspace clustering (FSC) algorithm," *Pattern Recognition*, vol. 41, no. 6, pp. 1939–1947, 2008.
- [65] R.-P. Li and M. Mukaidono, "A maximum-entropy approach to fuzzy clustering," in *Proceedings of 1995 IEEE International Conference on Fuzzy Systems*, vol. 4, 1995, pp. 2227–2232.
- [66] T. C. Havens, J. C. Bezdek, C. Leckie, L. O. Hall, and M. Palaniswami, "Fuzzy c-means algorithms for very large data," *IEEE Transactions on Fuzzy Systems*, vol. 20, no. 6, pp. 1130–1146, 2012.



Jun Wang (Life Fellow) received his B.S. and M.S. degrees in 1982 and 1985 from Dalian University of Technology, Dalian, China, and his Ph.D. degree in 1991 from Case Western Reserve University, Cleveland, Ohio, USA. He held various academic positions at Dalian University of Technology, Case Western Reserve University, University of North Dakota, and the Chinese University of Hong Kong, Hong Kong. He also held various short-term or part-time visiting positions at the U.S. Air Force Armstrong Laboratory, Dayton, Ohio, USA; RIKEN Brain Science Institute, Tokyo, Japan; Huazhong University of Science and Technology, Wuhan, China; Shanghai Jiao Tong University, Shanghai, China; Dalian University of Technology, Dalian, China; and Swinburne University of Technology, Melbourne, Australia. He is currently a chair professor at City University of Hong Kong, Hong Kong. He was a recipient of several awards such as the Research Excellence Award from the Chinese University of Hong Kong (2008–2009), Outstanding Achievement Award from Asia-Pacific Neural Network Assembly (2011), *IEEE Transactions on Neural Networks* Outstanding Paper Award (2011), Neural Networks Pioneer Award from the IEEE Computational Intelligence Society (2014), and Norbert Wiener Award from the IEEE Systems, Man and Cybernetics Society (2019). He served as the General Chair of the 13th/25th International Conference on Neural Information Processing (2006/2018) and the IEEE World Congress on Computational Intelligence (2008). He is an IEEE Systems, Man, and Cybernetics Society Distinguished Lecturer (2017–2022), was a Distinguished Lecturer of IEEE Computational Intelligence Society (2010–2012, 2014–2016). He was the Editor-in-Chief of the *IEEE Transactions on Cybernetics* (2014–2019).



Hongzong Li received the B.E. degree in automation from Northeastern University, Shenyang, Liaoning, China, in 2020. He is currently a Ph.D. candidate with the Department of Computer Science, City University of Hong Kong, Hong Kong. His current research interests include optimization, computational intelligence, and clustering.